Review and Evaluation of Lightning Return Stroke Models Including Some Aspects of Their Application

Vladimir A. Rakov, *Senior Member, IEEE*, and Martin A. Uman, *Fellow, IEEE*

***Abstract*—Four classes of models of the lightning return stroke are reviewed. These four classes are: 1) the gas dynamic models; 2) the electromagnetic models; 3) the distributed-circuit models; and 4) the "engineering" models. Validation of the reviewed models is discussed. For the gas dynamic models, validation is based on observations of the optical power and spectral output from natural lightning. The electromagnetic, distributed-circuit, and "engineering" models are most conveniently validated using measured electric and magnetic fields from natural and triggered lightning. Based on the entirety of the validation results and on mathematical simplicity, we rank the "engineering" models in the following descending order: MTLL, DU, MTLE, BG, and TL. When only the initial peak values of the channel-base current and remote electric or magnetic field are concerned, the TL model is preferred. Additionally discussed are several issues in lightning return-stroke modeling that either have been ignored to keep the modeling straightforward or have not been recognized, such as the treatment of the upper, in-cloud portion of the lightning channel, the boundary conditions at the ground, including the presence of a vertically extended strike object, the return-stroke speed at early times, the initial bi-directional extension of the return-stroke channel, and the relation between leader and return-stroke models. Various aspects of the calculation of lightning electric and magnetic fields in which return-stroke models are used to specify the source are considered, including equations for fields and channel-base current, as well as a discussion of channel tortuosity and branches.**

***Index Terms*—LEMP, lightning, modeling.**

I. Introduction

We define four classes of lightning return stroke models. Most published models can be assigned to one or sometimes two of these four classes. The classes are primarily distinguished by the type of governing equations.

1) The first class of models is the gas dynamic or "physical" models, which are primarily concerned with the radial evolution of a short segment of the lightning channel and its associated shock wave. These models typically involve the solution of three gas dynamic equations (sometimes called hydrodynamic equations) representing the conservation of mass, momentum, and energy, coupled to two equations of state with the input parameter being an assumed channel current versus time. Principal model outputs include temperature, pressure, and mass density as a function of radial coordinate and time.
2) The second class of models is the electromagnetic models that are usually based on a lossy, thin-wire antenna approximation to the lightning channel. These models involve a numerical solution of Maxwell's equations to find the current distribution along the channel from which the remote electric and magnetic fields can be computed.
3) The third class of models is the distributed-circuit models that can be viewed as an approximation to the electromagnetic models described above and that represent the lightning discharge as a transient process on a vertical transmission line characterized by resistance (R), inductance (L), and capacitance (C), all per unit length. The distributed-circuit models (also called R-L-C transmission-line models) are used to determine channel current versus time and height and can, therefore, also be used for the computation of remote electric and magnetic fields. Two distributed-circuit models incorporate a gas dynamic model with the latter being used to find R as a function of time.
4) The fourth class of models is the "engineering" models in which a spatial and temporal distribution of the channel current (or the channel-charge density) is specified based on such observed lightning return-stroke characteristics as current at the channel base, the speed of the upward-propagating front, and the channel luminosity profile. In these models, the physics of the lightning return stroke is deliberately downplayed and the emphasis is placed on achieving agreement between the model-predicted electromagnetic fields and those observed at distances from tens of meters to hundreds of kilometers. A characteristic feature of the "engineering" models is the small number of adjustable parameters, usually one or two besides the measured or assumed channel-base current.

Outputs of the electromagnetic, distributed-circuit, and "engineering" models can be directly used for the computation of electromagnetic fields, a primary electromagnetic compatibility (EMC) application of such models, while the gas dynamic models can be used for finding R as a function of time, which

Manuscript received September 15, 1998. This work was supported by NSF under grants ATM-9415507 (Program Director R. C. Taylor) and ATM-9726100 (Program Director S. P. Nelson).

The authors are with the Department of Electrical and Computer Engineering, University of Florida, Gainesville, FL 32611 USA.

Publisher Item Identifier S 0018-9375(98)08742-0.

is one of the parameters of the electromagnetic and distributed-circuit models. Since the distributed-circuit and "engineering" models generally do not consider lightning channel branches, they best describe subsequent strokes or first strokes before the first major branch has been reached by the upward-moving return stroke, a time that is usually longer than the time required for the formation of the initial current peak at ground. If not specified otherwise, we assume that the channel is straight and vertical and has no branches. Channel tortuosity, branches, and propagation effects are discussed in Section VII-F in relation to the calculation of electric and magnetic fields. The gas dynamic models are equally applicable to both first and subsequent strokes since they consider the radial evolution of a short segment of the channel. The electromagnetic models can be formulated for any channel geometry to represent either first or subsequent strokes.

In this review, we attempt to maintain a balance between emphasis on the primary features of modern lightning return stroke modeling and completeness. Thus, we do not consider several "engineering" models that are found in the previous literature, but are trivial special cases of the major models reviewed here (e.g., the Lundholm [1] or Norinder and Dahle [2] models) or that have been found to be impractical in view of more recent models (e.g., the Master–Uman–Lin–Standler (MULS) model [3]). As demonstrated by Rachidi and Nucci [4], the MTLE model (which we do discuss here) is essentially a more conveniently formulated equivalent of the MULS model that we do not include in this review. At the same time, we do include brief descriptions of several recently published models (most of them rather cumbersome to use) for the purpose of reflecting the scope of current efforts in lightning return stroke modeling. These include generalizations of the Diendorfer–Uman (DU) and traveling current source (TCS) models (Section V), Cooray's model (Section V), and an electromagnetic model of Borovsky (Section III).

II. Gas Dynamic Models

Gas dynamic models consider a short segment of a cylindrical plasma column driven by the resistive heating caused by a specified flow of electric current as a function of time. Some models of this type were developed for laboratory spark discharges in air but have been used for (e.g., Plooster [5]–[7]) or thought to be applicable to (e.g., Drabkina, [8], Braginskii, [9]) the lightning return stroke.

Drabkina [8], assuming the spark channel pressure to be much greater than the ambient pressure, described the radial evolution of a spark channel and its associated shock wave as a function of the time-dependent energy injected into the channel. Braginskii [9] also used this "strong-shock" approximation and developed a spark channel model describing parameters such as radius, temperature, and pressure as a function of the input current versus time. For a current $I(t)$ linearly increasing with time t, he gave the following expression for channel radius $r(t)$ (as presented by Plooster [7]): $r(t) \approx 9.35[I(t)]^{1/3}t^{1/2}$ where $r(t)$ is in centimeters, $I(t)$ in amperes, and t in seconds. In the derivation of this expression, presumably applicable to the early stages of the discharge, Braginskii [9] set the electrical conductivity σ of the channel at 2.22×10^4 S/m and assumed the ambient air density to be 1.29×10^{-3} g/cm^3. For a known $r(t)$, the resistance per unit channel length can be found as $R(t) = [\sigma\pi r^2(t)]^{-1}$ and the energy input per unit length as $w(t) = \int_0^t I^2(\tau)R(\tau)\,d\tau$.

More recent "physical" modeling algorithms, by Hill [10], [11], Plooster [5]–[7], Strawe [12], Paxton *et al*. [13], [14], Bizjaev *et al*. [15], and Dubovoy *et al*. [16]–[18], can be briefly outlined as follows. It is assumed that: 1) the plasma column is straight and cylindrically symmetrical; 2) the algebraic sum of positive and negative charges in any volume element is zero; and 3) local thermodynamic equilibrium exists at all times. Initial conditions that are meant to characterize the channel created by the lightning leader include temperature (of the order of 10 000°K), channel radius (of the order of 1 mm) and either pressure equal to ambient (1 atm) or mass density equal to ambient (of the order of 10^{-3} g/cm^3), the latter two conditions representing, respectively, the older and the newly created channel sections. The initial condition assuming ambient pressure probably best represents the upper part of the leader channel since that part has had sufficient time to expand and attain equilibrium with the surrounding atmosphere, while the initial condition assuming ambient density is more suitable for the recently created, bottom part of the leader channel. In the latter case, variations in the initial channel radius and initial temperature are claimed to have little influence on model predictions (e.g., Plooster [7], Dubovoy *et al*. [18]). The input current is assumed to rise to about 20 kA in some microseconds and then decay in some tens of microseconds. At each time step: 1) the electrical energy sources; 2) the radiation energy sources; and 3) sometimes the Lorentz force (Dubovoy *et al*. [16]–[18]), these three quantities being discussed in more detail below, are computed and the gas dynamic equations are numerically solved for the thermodynamic and flow parameters of the plasma. The exact form of the gas dynamic equations and the set of variables for which the equations are solved vary. Plooster [5]–[7], for instance, used five equations including equations of conservation of mass, momentum, and energy, a definition for the radial gas velocity, and an equation of state for the gas that were solved for the five variables: radial coordinate, radial velocity, pressure, mass density, and internal energy per unit mass.

1) Electrical Energy Sources: The electrical energy deposited into the channel is determined in the following manner. The plasma column is divided into a set of concentric annular zones, in each of which the gas properties are assumed constant. For known temperature and mass density, tables of computed properties of air in thermodynamic equilibrium (Hill [10], Dubovoy *et al*. [16]–[18]) or the Saha equation directly (Plooster [5]–[7], Paxton *et al*. [13], [14]) yield the plasma composition. Given the plasma composition, temperature, and mass density, one can compute the plasma conductivity for each of the annular zones. The total input current is apportioned to all of the annular zones as if they were an array of resistors connected in parallel. Using that cross-sectional distribution of current and plasma conductivity, one finds the electrical energy input (Joule heating) in each of the annular

zones. Most of this energy is spent for radiation, ionization, and expansion of the channel (Paxton *et al*. [13], [14]).

2) Radiation Energy Sources: The electrical energy deposited into the channel in the form of heat is transported from the hot conducting gas in the inner part of the channel to the cooler gas in the outer part of the channel. Radiation is the dominant mechanism of energy redistribution at temperatures above 10 000°K or so while thermal conduction is usually neglected (Paxton *et al*. [13], [14]). Radiative properties of air are complex functions of frequency and temperature. Radiation of a given frequency can be absorbed and reradiated a number of times in traversing the channel in the outward direction. Photons with wavelengths of 1000–2000 Å or shorter (e.g., UV) are absorbed right at the edge of the hot channel and contribute to enlarging the plasma column, while longer wavelength photons (mostly optical wavelengths) eventually escape from the system. Paxton *et al*. [13], [14] and Dubovoy *et al*. [16]–[18] used tables of radiative properties of hot air to determine absorption coefficients (opacities) as a function of temperature for a number of selected frequency (wavelength) intervals (for example, ten in Dubovoy *et al*. [16]–[18]), and solved the equation of radiative energy transfer in the diffusion approximation. Less detailed radiative transport algorithms have also been employed (Hill [10], Plooster [6]–[7], Strawe [12]).

3) Lorentz Force: In their model, Dubovoy *et al*. [16]–[18] included the pinch effect due to the interaction of a current with its own magnetic field. They computed the Lorenz force from the input current, the previously calculated plasma conductivity, a point form of Ohm's law and Ampere's law and they included this force, which is directed toward the axis of the channel and counteracts the channel's gas dynamic expansion, in the momentum and energy conservation equations. Inclusion of the interaction of the channel current with its own magnetic field is claimed to result in a 10–20% increase in the input energy for the same input current.

Perhaps the most advanced and completely presented gas dynamic model to date is that of Paxton *et al*. [13], [14]. The results of Paxton *et al*. [13], [14] including temperature, pressure, mass density, and electrical conductivity versus radial coordinate at different instants of time are shown in Figs. 1–4. Return stroke input energy estimates predicted by various "physical" models as well as an estimate of Krider *et al*. [19] (from comparison of the optical radiation produced by lightning with that of a laboratory spark of known input energy) and estimates based on the electrostatic considerations of Uman [20] and Borovsky [21] are summarized in Table I. Additionally, the percentages of the input energy converted to kinetic energy of gas motion (shock wave and conducting channel expansion) and of the energy radiated from the channel are given for some models.

As noted earlier, the gas dynamic models do not consider the longitudinal evolution of the lightning channel. They also usually ignore the electromagnetic skin effect (found to be negligible by Plooster [6]), the corona sheath, which presumably contains the bulk of the leader charge, and any heating of the air surrounding the current-carrying channel by preceding lightning processes. An attempt to include the

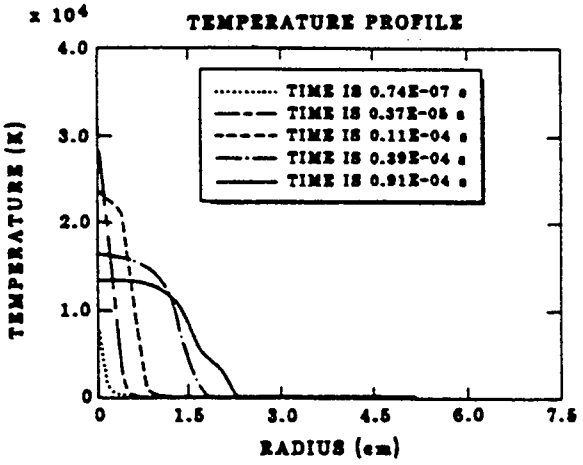

Fig. 1. Temperature versus radius (radial distance from channel axis) at five instants of time ranging from 0.074 to 91 μs as predicted by the gas dynamic model of Paxton *et al*. [13], [14] for an input current linearly rising to 20 kA in 5 μs and thereafter exponentially decaying with a time constant of 50 μs. The profile at 3.7 μs should be interpreted as having a constant value equal to that at the channel axis out to a radius of 0.36 cm (Paxton *et al*. [68]). Adapted from Paxton *et al*. [13], [14].

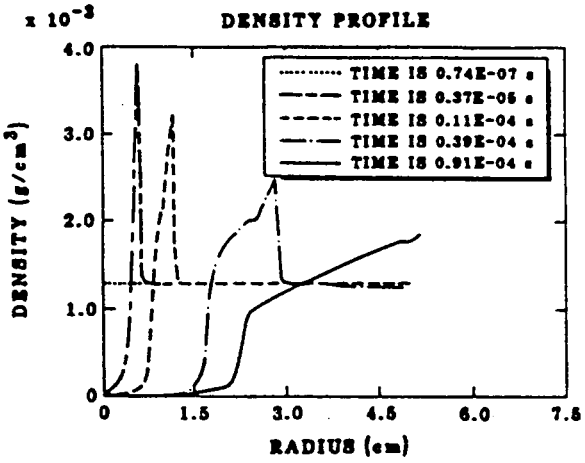

Fig. 2. Same as Fig. 1 but for mass density profiles.

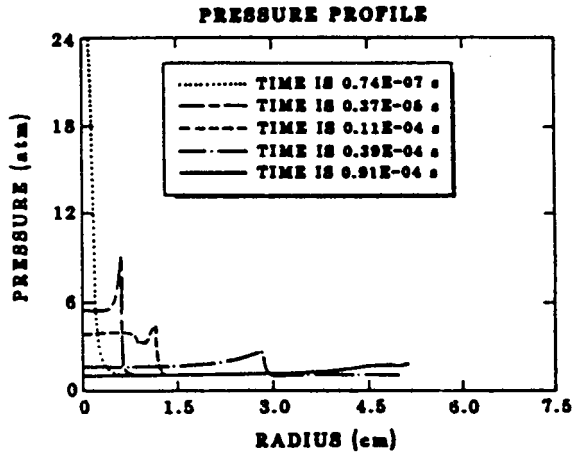

Fig. 3. Same as Fig. 1 but for pressure profiles.

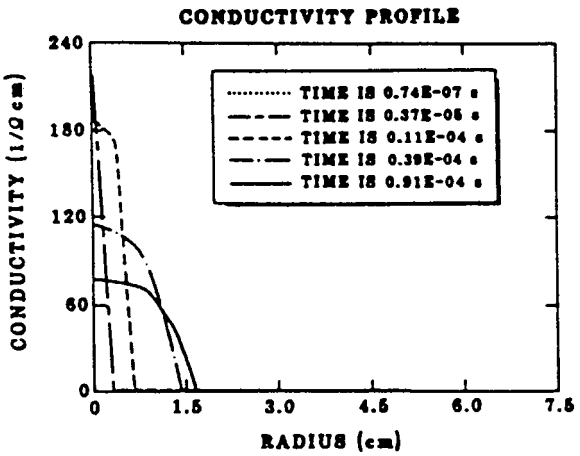

Fig. 4. Same as Fig. 1 but for electrical conductivity profiles.

previous heating in a gas dynamic model was made by Bizjaev *et al.* [15].

III. Electromagnetic Models

Electromagnetic return-stroke models based on the representation of the lightning channel as a lossy antenna have been proposed by Podgorski and Landt [22] and Moini *et al.* [23]. These models involve a numerical solution of Maxwell's equations using the method of moments (MoM) (e.g., Sadiku [24]), which yields the complete solution for channel current including both the antenna-mode current and the transmission-line-mode current (e.g., Paul [25]). The resistive loading used in [22] was 0.7 Ω/m and that used in [23] was 0.065 Ω/m. In order to simulate the effect on the return-stroke velocity of the radially formed corona surrounding the current-carrying channel core and presumably containing the bulk of the channel charge, Moini *et al.* [23] set the permittivity ε of the air surrounding the equivalent antenna to a value greater than ε_0 for the computation of the current distribution along the antenna. As a result, even without resistive loading, the phase velocity of an electromagnetic wave guided by the antenna $v_p = (\mu_0\varepsilon)^{-1/2}$ was reduced with respect to the velocity of light $c = (\mu_0\varepsilon_0)^{-1/2}$. The resistive loading further reduced v_p. The current distribution computed assuming the surrounding air had permittivity ε and the antenna was resistively loaded was then allowed to radiate electromagnetic fields into free-space characterized by $\varepsilon = \varepsilon_0$, $\mu = \mu_0$. The model of Moini *et al.* [23] considers a straight vertical channel, while the model of Podgorski and Landt [22] deals with a three-dimensional (3-D) channel of arbitrary shape and reportedly can include branches, strike objects, upward connecting discharges, and nonlinear effects during the attachment process.

Borovsky [26] used Maxwell's equations to describe both dart-leader and return-stroke processes as guided waves propagating along conducting cylindrical channels. The resistance per unit length of the channel guiding the return-stroke wave was assumed to be 16 Ω/m. No current distribution along the channel was calculated since the dart leader and return stroke were each represented by a single dominant sinusoid and only a middle section of the lightning channel, undisturbed by the conditions at the channel ends, was considered.

IV. Distributed-Circuit Models

Distributed-circuit models consider the lightning channel to be an R-L-C transmission line for which voltage V and current I are solutions of the telegrapher's equations

$$-\frac{\partial V(z',t)}{\partial z'} = L\frac{\partial I(z',t)}{\partial t} + RI(z',t) \tag{1}$$

$$-\frac{\partial I(z',t)}{\partial z'} = C\frac{\partial V(z',t)}{\partial t'} \tag{2}$$

where R, L, and C are, respectively, the series resistance, series inductance, and shunt capacitance, all per unit length, z' is the vertical coordinate specifying position on the lightning channel, and t is the time. The equivalent transmission line is usually assumed to be charged (by the preceding leader) to a specified potential and then closed at the ground end with a specified earth resistance to initiate the return stroke. The second of the telegrapher's equations is equivalent to the continuity equation. Equations (1) and (2) can be derived from Maxwell's equations assuming that the electromagnetic waves propagating on (guided by) the line exhibit a quasi-TEM field structure and that R, L, and C are constant (e.g., Agrawal *et al.* [27]). Note that the term "quasi-TEM field structure" implies that the transverse component of the total electric field is much greater than the z-directed component associated with a nonzero value of R (Paul [25]). The telegrapher's equations can be also derived using Kirchhoff's laws (e.g., Sadiku [24]) from the equivalent circuit shown in Fig. 5. In general, each of the transmission line parameters representing a return-stroke channel is a function of time and space; that is, the transmission line is nonlinear and nonuniform (e.g., Rakov [28]). The channel inductance changes with time due to variation in the radius of the channel core that carries the z-directed channel current. The channel resistance changes with time due to variation in the electron density, heavy particle density, and the radius of the channel core. The channel capacitance changes with time mostly due to the neutralization of the radially formed corona sheath that surrounds the channel core and presumably contains the bulk of the channel charge deposited by the preceding leader. For the case of a nonlinear transmission line, (1) and (2) are still valid if L and C are understood to be the dynamic (as opposed to the static) inductance and capacitance, respectively (e.g., Gorin [29]): $L = \partial\phi/\partial I$, $C = \partial\rho/\partial V$ where ϕ is the magnetic flux linking the channel and ρ is the channel charge, both per unit length.

An exact closed-form solution of the telegrapher's equations can be generally obtained only in the case of R, L, and C all being constant. There is at least one exception to this latter statement: a nonlinear distributed-circuit model described in [30] and [31] in which C is a function of charge density to simulate the radial-corona sheath. The telegrapher's equations representing this model admit exact solutions but only if $R = 0$. Linear distributed-circuit models have been used, for instance, by Oetzel [32], Price and Pierce [33] ($R \approx 0.06$ Ω/m), Little [34] ($R = 1$ Ω/m), and Takagi and Takeuti [35] ($R = 0.08$ Ω/m). Rakov [28] found that the behavior of electromagnetic waves guided by a linear R-L-C transmission line representing the prereturn-stroke channel formed by a dart leader and having $R = 3.5$ Ω/m is consistent with the observed

TABLE I
LIGHTNING ENERGY ESTIMATES

Source	Current Peak, kA	Input Energy, J/m	Percent Converted to Kinetic Energy	Percent of Energy Radiated	Comments
Hill [10, 11]	21	1.5×10^4 ($\sim3\times10^3$)	9† (at 25 μs)	~2*† (at 25 μs)	Underestimation of electrical conductivity resulted in a factor of 5 or so overestimation of input energy. Corrected value is given in parentheses
Plooster [7]	20	2.4×10^3	4 (at 35 μs)	~50 (at 35 μs)	Crude radiative transport mechanism adjusted to expected temperature profile
Paxton et al. [13, 14]	20	4×10^3	2 (at 64 μs)	69 (at 64 μs)	Individual temperature-dependent opacities for several wavelength intervals
Dubovoy et al. [16-18]	20	3×10^3	-	25 (at ≳55 μs)	Individual temperature-dependent opacities for ten wavelength intervals. Magnetic pinch effect is taken into account
Borovsky [21]	-	2×10^2-1×10^4	-	-	Electrostatic energy stored on a vertical channel assuming a line charge density of 100-500 μC/m
Krider et al. [19]	Single-stroke flash	2.3×10^5	-	0.38#	Measured optical energy is converted to the total energy using energy ratios observed in laboratory spark experiments
Uman [20]	-	$(2\text{-}20)\times10^5$	-	-	From electrostatic considerations (lowering tens of coulombs from a height of 5 km to ground, assuming a potential difference of 10^8-10^9 V between the Earth and the charge center)

*Estimated by subtraction of the internal and kinetic energies from the input energy shown in Fig. 1 of *Hill* [11].
† Probably incorrect due to a factor of 20-30 error in electrical conductivity.
#Only radiation in the wavelength region from 0.4 to 1.1 μm.

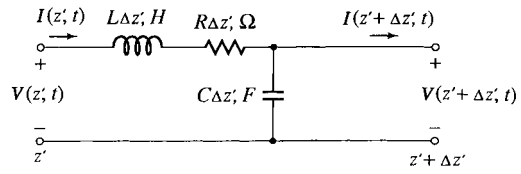

Fig. 5. The equivalent circuit for an elemental section of an R-L-C transmission line from which the telegrapher's equations (1) and (2) can be derived using Kirchhoff's laws in the limit as $\Delta z' \rightarrow 0$. In general, the transmission-line parameters R, L, and C, are each a function of z' and t. The return path corresponds to the lightning channel image (assuming a perfectly conducting ground). All the information on the actual geometry of the transmission line is contained in L and C.

luminosity profiles for the return stroke (Jordan and Uman [36]). If the line nonlinearities are taken into account, the solution of the telegrapher's equations requires the use of a numerical technique, for instance, a finite-difference method (Quinn [37]). Attempts to take into account the lightning channel nonlinearities using various simplifying assumption have been made by Bazelyan *et al.* [38], Gorin [29], Baum and Baker [30], Baum [31], Mattos and Christopoulos [39], [40], and Kostenko [41]. The results presented by Bazelyan *et al.* [38] are shown as an example in Figs. 6 and 7.

Even if R, L, and C were constant, the application of the R-L-C transmission line model to lightning is an approximation. Indeed, for a vertical lightning channel with the current "return path" being the channel image (assuming a perfectly conducting ground) the validity of the TEM assumption is questionable, in particular, near the return-stroke tip where a relatively large longitudinal component of electric field is present. Usually, a distributed-circuit model of the lightning return stroke is postulated without proper analysis of its applicability. Baum and Baker [30] represented the lightning channel "return path" by a cylinder coaxial with and enclosing the lightning channel. They do not give any proof of the equivalency of such a coaxial system to the actual configuration of a lightning channel and its image. Clearly, the radius of the artificial outer return-path cylinder affects the L and C values of such a coaxial R-L-C transmission line model. Note that the telegrapher's equations (1) and (2) are the same for any two-conductor line (including a coaxial one), with all the information on the actual line geometry being contained in L and C.

Strawe [12] proposed two versions of a distributed-circuit model that differ in the way that the value of R as a function of channel current and channel electrical conductivity was computed. In the first version, the conductivity was assumed

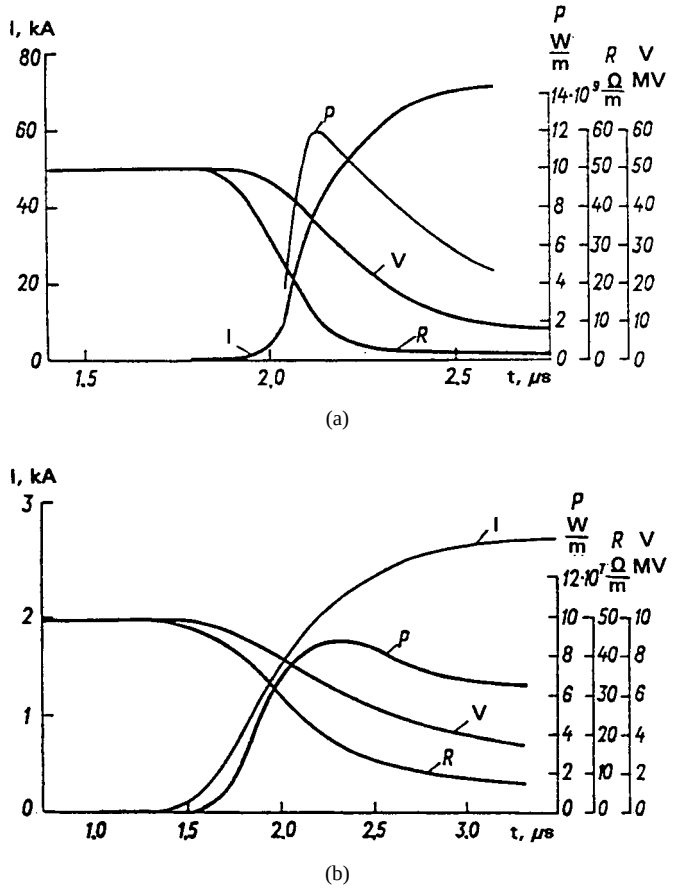

Fig. 6. Current I, voltage V, power per unit length P, and resistance per unit length R as a function of time t at a height of 300 m above ground as predicted by the distributed-circuit model of Bazelyan *et al.* [38]. Profiles are given for (a) $V_0 = 50$ MV and an instantaneously discharged corona sheath and for (b) $V_0 = 10$ MV and no corona sheath where V_0 is the initial uniform voltage on the channel due to charges deposited by the preceding leader. Adapted from Bazelyan *et al.* [38].

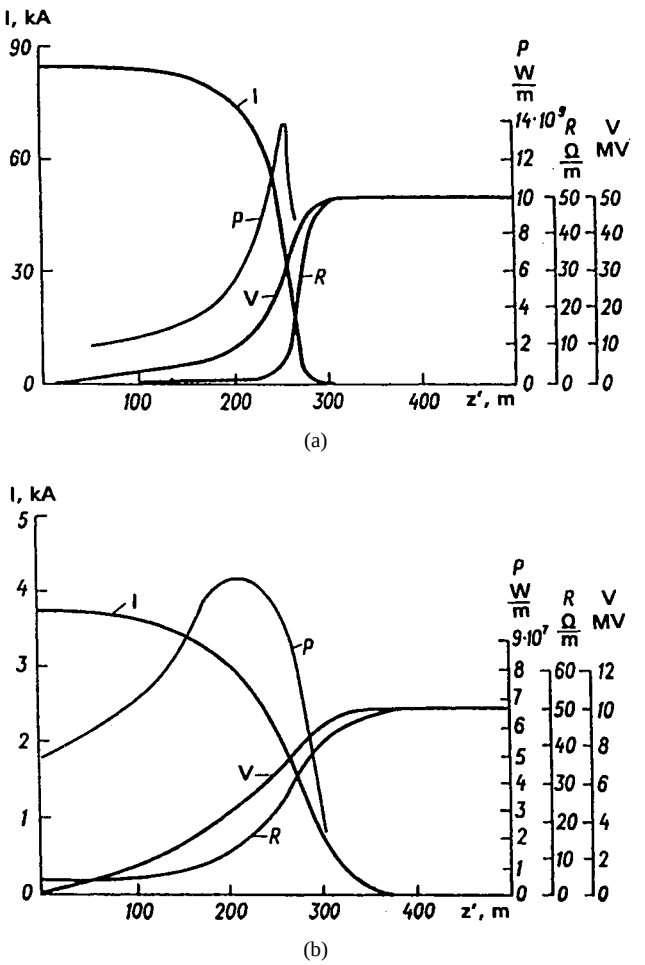

Fig. 7. Same as Fig. 6 but as a function of height z' along the channel at a given instant of time.

to be constant so that R varied only because of channel expansion. In the second version, the conductivity was a function of channel temperature and pressure that were found using a model of the gas dynamic type. In both versions, L and C were assumed constant. An upward-going connecting discharge from earth of 100-m length was simulated as an R-L-C transmission line as well. The second version of Strawe's [12] model is actually a combination of a gas dynamic model and a distributed-circuit model. A combination of a gas dynamic model (although not described in detail) and a distributed-circuit model was also proposed by Baker [42].

V. "Engineering" Models

An "engineering" return-stroke model is defined in this review as an equation relating the longitudinal channel current $I(z',t)$ at any height z' and any time t to the current $I(0,t)$ at the channel origin ($z' = 0$). An equivalent expression in terms of the line charge density $\rho(z',t)$ on the channel can be obtained using the continuity equation (Thottappillil *et al.* [43]). Thottappillil *et al.* [43] distinguished between two components of the charge density at a given channel section, one component being associated with the return-stroke charge transferred through this channel section and the other with the charge deposited at this channel section. As a result, their charge density formulation provides new insights into the physical mechanisms behind the models, generally not recognized in the longitudinal-current formulation.

We first consider mathematical and graphical representations of some simple models and then categorize and discuss the most used "engineering" models based on their implications regarding the principal mechanism of the return-stroke process. A number of simple "engineering" models can be expressed by the following (Rakov [44]):

$$I(z',t) = u(t - z'/v_f)P(z')I(0, t - z'/v) \tag{3}$$

where u is the Heaviside function equal to unity for $t \geq z'/v_f$ and zero otherwise, $P(z')$ is the height-dependent current attenuation factor introduced by Rakov and Dulzon [45], v_f is the upward-propagating front speed (also called return-stroke speed), and v is the current-wave propagation speed. Table II summarizes $P(z')$ and v for five "engineering" models, namely, the transmission line model TL [46] (not to be confused with the R-L-C transmission line models discussed above); the modified transmission-line model with linear current decay with height MTLL [47]; the modified transmission line model with exponential current decay with

TABLE II
$P(z')$ AND v IN (3) FOR FIVE SIMPLE "ENGINEERING" MODELS. ADAPTED FROM RAKOV [44]

Model	P(z′)	v
TL (*Uman and McLain* [46])	1	v_f
MTLL (*Rakov and Dulzon* [47])	1 - z′/H	v_f
MTLE (*Nucci et al.*[48])	exp(-z′/λ)	v_f
BG (*Bruce and Golde* [49])	1	∞
TCS (*Heidler* [50])	1	-c

height MTLE [48]; the Bruce-Golde model BG [49]; and the traveling current source model TCS [50]. In Table II, H is the total channel height, λ is the current decay constant (assumed by Nucci *et al*. [48] to be 2000 m) and c is the speed of light. If not specified otherwise, v_f is assumed to be constant. Front speeds decaying exponentially with time, which is equivalent to decaying linearly with height (as shown by Leise and Taylor [52]), have also been used in an attempt to model the first stroke in a flash (e.g., Bruce and Golde [49]; Uman and McLain [46]; Dulzon and Rakov [52]). The three simplest models, TCS, BG, and TL, are illustrated in Fig. 8 and the TCS and TL models additionally in Fig. 9. We consider first Fig. 8. For all three models we assume the same current waveform at the channel base $(z' = 0)$ and the same front speed represented in the $z' - t$ coordinates by the slanted line labeled v_f. The current-wave speed is represented by the line labeled v, which coincides with the vertical axis for the BG model and with the v_f line for the TL model. Shown for each model are current versus time waveforms at the channel base $(z' = 0)$ and at heights z'_1 and z'_2. Because of the finite front propagation speed v_f, current at a height, say z'_2, begins with a delay z'_2/v_f with respect to the current at the channel base. The dark portion of the waveform indicates current that actually flows through a given channel section, the blank portion being shown for illustrative purpose only. As seen in Fig. 8, the TCS, BG, and TL models are characterized by different current profiles along the channel, the difference being, from a mathematical point of view, due to the use of different values of v (listed in Table II) in the generalized equation (3) with $P(z') = 1$. It also follows from Fig. 8 that if the channel-base current were a step function, the TCS, BG, and TL models would be characterized by the same current profile along the channel, although established in an apparently different way in each of the three models. The relation between the TL and TCS models is further illustrated in Fig. 9, which shows that the spatial current wave moves in the positive z' direction for the TL model and in the negative z' direction for the TCS model. Note that in Fig. 9 current at ground $(z' = 0)$ and upward moving front speed v_f are the same for both TL and TCS models. As in Fig. 8, the dark portion of the waveform indicates current that actually flows in the channel, the blank portion being shown for illustrative purpose only.

The most used "engineering" models can be grouped in two categories: the transmission-line-type models and the traveling-current-source-type models, summarized in Tables III and IV, respectively. Each model in Tables III and IV is represented by both current and charge density equations. Table III includes the TL model and its two modifications: the MTLL and MTLE models. Rakov and Dulzon [45] additionally considered modified transmission line models with current attenuation factors other than the linear and exponential functions used in the MTLL and MTLE models, respectively. The transmission-line-type models can be viewed as incorporating a current source at the channel base, which injects a specified current wave into the channel, that wave propagating upward: 1) without either distortion or attenuation (TL) or 2) without distortion but with specified attenuation (MTLL and MTLE), as seen from the corresponding current equations given in Table III.

Table IV includes the BG model [49], the TCS model [50], and the Diendorfer–Uman (DU) model [53]. In the traveling-current-source-type models, the return-stroke current may be viewed as generated at the upward-moving return-stroke front and propagating downward. In the TCS model, current at a given channel section turns on instantaneously as this section is passed by the front, while in the DU model, current turns on gradually (exponentially with a time constant τ_D if $I(0, t + z'/c)$ were a step function). Channel current in the TCS model may be viewed as a downward-propagating wave originating at the upward-moving front, as illustrated in Fig. 9. The DU model formulated in terms of current involves two terms (see Table IV), one being the same as the downward-propagating current in the TCS model that exhibits an inherent discontinuity at the upward-moving front (see Fig. 8), and the other one being an opposite polarity current which rises instantaneously to the value equal in magnitude to the current at the front and then decays exponentially with a time constant τ_D. The second current component in the DU model, which may be viewed merely as a front modifier, propagates upward with the front and eliminates any current discontinuity at that front. Time constant τ_D is the time during which the charge per unit length deposited at a given channel section by the preceding leader reduces to $1/e$ (about 37%) of its original value after this channel section is passed by the upward-moving front. Thottappillil and Uman [78] and Thottappillil *et al*. [43] assumed that $\tau_D = 0.1$ μs. Diendorfer and Uman [53] considered two components of charge density each released with its own time constant in order to match model predicted fields with measured fields. If $\tau_D = 0$, the DU model reduces to the TCS model. In both the TCS and DU models, current propagates downward at the speed of light. The TCS model reduces to the BG model if the downward current propagation speed is set equal to infinity instead of the speed of light. Although the BG model could be also viewed mathematically as a special case of the TL model with v replaced by infinity, we choose to include the BG model in the traveling-current-source-type model category. Thottappillil *et al*. [54] mathematically generalized the DU model to include

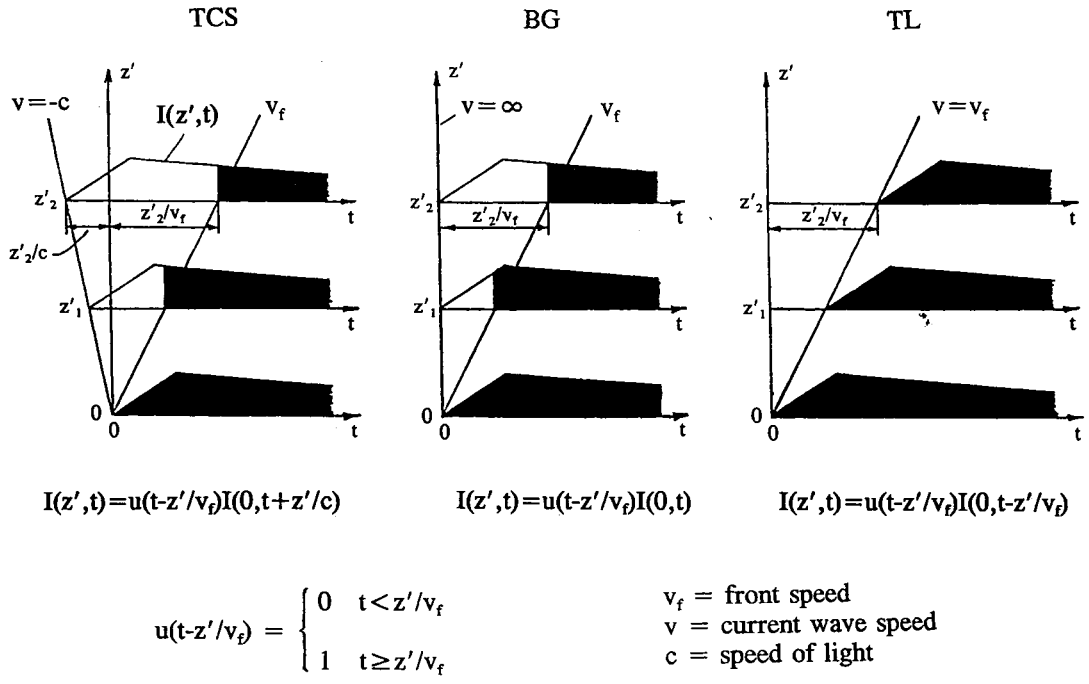

Fig. 8. Current versus time waveforms at ground ($z' = 0$) and at two heights z'_1 and z'_2 above ground for the TCS, BG, and TL return-stroke models. Slanted lines labeled v_f represent upward speed of the return-stroke front and lines labeled v represent speed of the return-stroke current wave. The dark portion of the waveform indicates current that actually flows through a given channel section. Note that the current waveform at $z' = 0$ and v_f are the same for all three models. Adapted from Rakov [44].

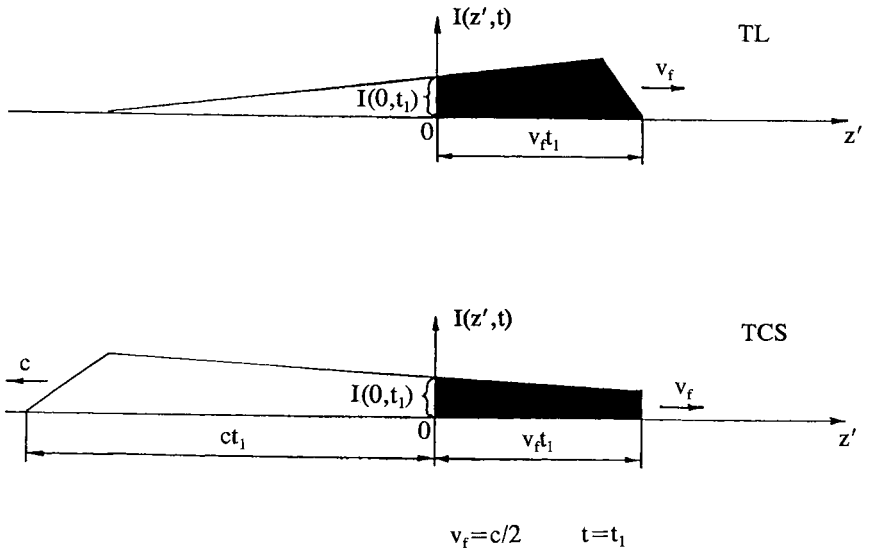

Fig. 9. Current versus height z' above ground at an arbitrary fixed instant of time $t = t_1$ for the TL and TCS models. Note that the current at $z' = 0$ and v_f are the same for both the models. Adapted from Rakov [44].

a variable upward front speed and a variable downward current wave speed, both separate arbitrary functions of height (this model was dubbed MDU where M stands for "modified"). A further generalization of the DU model (Thottappillil and Uman [55]) involves a single height-variable time constant τ_D. Generalizations of the TCS model are discussed later in this section.

The principal distinction between the two types of the "engineering" models formulated in terms of current is the direction of the propagation of current wave: upward for the transmission-line-type models $(v = v_f)$ and downward for the traveling-current-source-type models $(v = -c)$ as seen for the TL and TCS models, respectively, in Fig. 9. As noted earlier, the BG model can be viewed mathematically as a special case of either TCS or TL model. The BG model includes a current wave propagating at an infinitely large speed and, as a result, the wave's direction of propagation is indeterminate. As all other models, the BG model includes a front moving at a finite speed v_f. Note that, even though the direction of propagation of the current wave in a model can be either up or down, the

TABLE III
TRANSMISSION-LINE-TYPE MODELS FOR $t \geq z'/v_f$

TL (*Uman and McLain* [46])	$I(z',t) = I(0,t - z'/v)$ $\rho_L(z',t) = \frac{I(0,t-z'/v)}{v}$
MTLL (*Rakov and Dulzon* [47])	$I(z',t) = \left(1 - \frac{z'}{H}\right) I(0,t-z'/v)$ $\rho_L(z',t) = \left(1 - \frac{z'}{H}\right) \frac{I(0,t-z'/v)}{v} + \frac{Q(z',t)}{H}$
MTLE (*Nucci et al.* [48])	$I(z',t) = e^{-z'/\lambda} I(0,t-z'/v)$ $\rho_L(z',t) = e^{-z'/\lambda} \frac{I(0,t-z'/v)}{v} + \frac{e^{-z'/\lambda}}{\lambda} Q(z',t)$

$Q(z',t) = \int_{z'/v}^{t} I(0,\tau - z'/v)d\tau$ $\quad v = v_f = \text{const}$ $\quad H = \text{const}$ $\quad \lambda = \text{const}$

TABLE IV
TRAVELING-CURRENT-SOURCE-TYPE MODELS FOR $t \geq z'/v_f$

BG (*Bruce and Golde* [49])	$I(z',t) = I(0,t)$ $\rho_L(z',t) = \frac{I(0,z'/v_f)}{v_f}$
TCS (*Heidler* [50])	$I(z',t) = I(0,t+z'/c)$ $\rho_L(z',t) = -\frac{I(0,t+z'/c)}{c} + \frac{I(0,z'/v^*)}{v^*}$
DU *Diendorfer and Uman* [53])	$I(z',t) = I(0,t+z'/c) - I(0,z'/v^*)e^{-(t-z'/v_f)/\tau_D}$ $\rho_L(z',t) = -\frac{I(0,t+z'/c)}{c} - \left[\frac{I(0,z'/v^*)}{v_f} + \frac{\tau_D}{v^*}\frac{dI(0,z'/v^*)}{dt}\right] e^{-(t-z'/v_f)/\tau_D} + \frac{I(0,z'/v^*)}{v^*} + \frac{\tau_D}{v^*}\frac{dI(0,z'/v^*)}{dt}$

$v^* = v_f/(1+v_f/c)$ $\quad v_f = \text{const}$ $\quad \tau_D = \text{const}$

direction of current is the same; that is, charge of the same sign is effectively transported to ground in both types of the "engineering" models.

The TL model predicts (e.g., Uman *et al*. [56]) that, as long as: 1) the height above ground of the upward-moving return-stroke front (as "seen" at the observation point) is much smaller than the distance r between the observation point on ground and the channel base so that all contributing channel points are essentially equidistant from the observer; 2) the return-stroke front propagates at a constant speed; 3) the return-stroke front has not reached the top of the channel; and 4) the ground conductivity is high enough so that propagation effects (Section VIII-D) are negligible, the vertical component E_z^{rad} of the electric radiation field (and the horizontal component of the magnetic radiation field) is proportional to the channel-base current I. The equation for the electric radiation field E_z^{rad} is as follows:

$$E_z^{\text{rad}}(r,t) = -\frac{v}{2\pi\varepsilon_0 c^2 r} I(0,t-r/c) \tag{4}$$

where ε_0 is the permittivity of free-space, v is the upward propagation speed of the current wave, which is the same as the front speed v_f in the TL as well as in the MTLL and MTLE models, and c is the speed of light. For the most common return stroke lowering negative charge to ground, the sense of positive charge flow is upward so that current I, assumed to

be upward-directed in deriving (4) is, by convention, positive and $E_z^{\rm rad}$ by (4) is negative; that is, the electric field vector points in the negative z direction. Taking the derivative of this equation with respect to time, one obtains

$$\frac{\partial E_z^{\rm rad}(r,t)}{\partial t} = -\frac{v}{2\pi\varepsilon_0 c^2 r}\frac{\partial I(0,t-r/c)}{\partial t}. \tag{5}$$

These two equations are commonly used, particularly the first one and its magnetic radiation field counterpart found from $|B_\phi^{\rm rad}| = |E_z^{\rm rad}|/c$, for the estimation of the peak values of return-stroke current and its time derivative, subject to the assumptions listed prior to (4). Equations (4) and (5) have been used (as further discussed in Section VII-C) for the estimation of v from measured E_p/I_p and $(dE/dt)_p/(dI/dt)_p$, respectively, where the subscript "z" and superscript "rad" are dropped and the subscript "p" refers to peak values. The expressions relating channel base current and electric radiation field far from the channel for the BG, TCS, and MTLE models are given by Nucci *et al.* [57]. General equations for computing electric and magnetic fields at ground are considered in Section VIII-A.

As stated in Section I, a characteristic feature of the "engineering" models is the small number of adjustable parameters, usually one or two besides the channel-base current. In these models, the physics of the lightning return stroke is deliberately downplayed and the emphasis is placed on achieving an agreement between model-predicted electromagnetic fields and those observed at distances from tens of meters to hundred of kilometers.

In the rest of this section, we will briefly describe Cooray's [58] model and generalizations of the TCS model by Heidler and Hopf [59]–[61] and by Cvetic and Stanic [62], although most of these models do not belong to the "engineering" model class as defined at the beginning of this section.

Cooray [58] proposed a model that can be viewed as a "what if"-type model, since it contains a large number of adjustable parameters, many of them being presently unknown. In this model, a charge density distribution along the channel at $t = 0$ is specified separately for the inner part of the channel (the channel core and the so-called hot-corona sheath) and for the outer part of the channel (the so-called cold-corona sheath). Four adjustable parameters are used. Further, the dynamics of the charge release by the return-stroke front is assumed and involves four more adjustable parameters. The return-stroke speed profile is predicted by the model (as opposed to the "engineering" models in which it is specified on the basis of optical measurements) but requires one more adjustable parameter: longitudinal electric field intensity in the prereturn-stroke channel. It is not clear if Cooray's [58] model, which includes a total of nine adjustable parameters, is an improvement on the "engineering" models from the standpoint of the model-predicted electromagnetic fields. The charge density distribution along the channel in Cooray's [58] model is described by the sum of two exponential functions and near ground is not much different from the single-exponential-function distribution in the MTLE model. Therefore, we might expect that like the MTLE model Cooray's [58] model is not capable of the reproduction of the electric fields measured tens of meters from triggered-lightning return strokes (see Section VI-D).

Heidler and Hopf [59] modified the TCS model to take into account wave reflections at ground and at the upward-moving front using the traveling-current source current as an input to the model. The source current is the current associated with the upward-moving front, which can be viewed as derived from the charge density distribution deposited along the channel by the preceding leader (e.g., Thottappillil *et al.* [43]). Both upward and downward waves behind the upward-moving front propagate at the speed of light, and the resultant reflection coefficient at the front is a function of v_f and c. The channel-base current in this model depends on the reflection coefficient at the strike point and on the initial charge density distribution along the channel. Heidler and Hopf [60] further modified the TCS model expressing the source current and, therefore, the initial charge density distribution along the channel, in terms of the channel-base current and current reflection coefficient at ground. Interestingly, inclusion of current reflections at ground and at the upward-moving front in the TCS model resulted in a decrease of the initial electric field peak and maximum field derivative at 10 km [61]. Cvetic and Stanic [62] proposed a model from which the TCS and DU models can be derived as special cases. Within the concept of the TCS model, they specify independently the channel-base current and the initial charge density distribution along the channel. The resultant current distribution along the channel is determined using the equation of current continuity.

VI. Model Validation

A. Gas Dynamic Models

Attempts to validate the gas dynamic models have been made by comparing their predictions with: 1) the temperature, electron density, and pressure profiles published by Orville [63]–[65]; 2) the radiated optical power determined by Guo and Krider [66], [67]; and 3) the input electrical energy of the return stroke estimated by Krider *et al.* [19].

From an analysis of ten time-resolved spectra of return strokes, Orville [64] obtained channel temperature and electron density, each as a function of time. Typical peak temperatures, determined from ratios of intensities of spectral lines were of the order of 28 000–31 000°K. No temperatures exceeded 36 000°K. In two of the ten strokes, temperature appeared to rise to a peak value during the first 10 μs (time resolution was 5 μs) and to decay thereafter. In the remaining eight strokes (including two with 2-μs time resolution), temperature decreased monotonically. The electron density, determined from the Stark broadening of the H_α line, was 8×10^{17} cm^{-3} in the first 5 μs, decreasing to 1–1.5 $\times$ 10^{17} cm^{-3} at 25 μs, and remaining approximately constant to 50 μs. Additionally, using Gilmore's tables for the composition of dry air in thermodynamic equilibrium, Orville [65] found that the channel is characterized by an average pressure of 8 atm (1atm $= 10^5 N/m^2$) in the first 5 μs and attains atmospheric pressure at approximately 20 μs. Hill [10, fig. 1], Plooster [7, fig. 1], and Paxton *et al.* [14, p. 56, fig. 8] showed that

their model-predicted temperature versus time curves were generally consistent with those of Orville [64]. Plooster [7, figs. 2, 3] did so also for electron density and pressure. Paxton *et al*. [14, fig. 8] is reproduced in Fig. 1 here.

Guo and Krider [66], [67], using a photoelectric detector, found the time and space averaged mean radiance in the 0.4 to 1.1-μm wavelength range (essentially optical power) for first strokes to be of the order of 10^6 W/m. Paxton *et al*. [13], [14] computed, using their model and current waveform with a peak of 20 kA, the average (over the first 10 μs) radiated optical power in the 0.4–1.2-μm range to be essentially equal to that value.

Using the measured optical radiated energy in the wavelength region from 0.4 to 1.1 μm from a single-stroke lightning of 870 J/m and that from a long laboratory spark of known input energy, Krider *et al*. [19] have deduced the input energy for lightning to be 2.3×10^5 J/m. The percentage of total energy that is optically radiated from the channel is 0.38% according to Krider *et al*. [19]. The gas dynamic models predict (see Table I) lightning input energy values about two orders of magnitude lower than the value deduced by Krider *et al*. [19] and percentages of radiated energy comparably higher. For example, Dubovoy *et al*. [16]–[18] computed for a 20 kA return stroke that the energy lost (after 55 μs or so) by radiative processes was 700 J/m which is roughly 25% of the input energy of 3×10^3 J/m computed by them. It is important to note that the relatively high energy value of 1.5×10^4 J/m reported by Hill [10] is an overestimate because he used an equation for the electron-neutral collision frequency that is invalid for the most important temperature range from 8000 to 30 000°K, as pointed out by both Paxton *et al*. [68] and Dubovoy *et al*. [16]–[18]. As a result, Hill's [10] values of channel electrical conductivity are 20–30 times lower than observed experimentally in this temperature range, leading to the erroneous value of input energy. Since the input energy varies roughly as the inverse square root of the conductivity (Plooster [6]), the corrected value of energy for Hill's [10] model is about 3×10^3 J/m, in keeping with values predicted by other gas dynamic models (see Table I). Note that other results of Hill [10] (e.g., the commonly quoted pressure versus radius and time (Uman [20, fig. 15.11]) must be affected by his error in conductivity computations and, therefore, should be considered in need of correction as well. Thus, there exists about a two order of magnitude discrepancy between the lightning input energy predicted by the gas dynamic models and that deduced by Krider *et al*. [19] from comparison with long laboratory spark studies. This disparity remains a subject of controversy. Plooster [7], in particular, argues that with the channel electrical conductivity near 2×10^4 S/m, the radius of the conducting channel would have to be less than 0.15 cm for the entire duration of the current waveform to give a total energy input of 10^5 J/m, instead of rapidly increasing by an order of magnitude or so. Paxton *et al*. [13], [14] view Plooster's [7] argument as strong evidence for 10^5 J/m being a significant overestimate of lightning energy. Further, input energy predicted by the gas dynamic models appears to be consistent with the estimate of Borovsky [21] based on the computation of electrostatic energy stored on a lightning channel assuming a line charge density of 100–500 μC/m (see Table I). Finally, according to Hill [11], only one thirtieth of the input electrical energy supplied to the spark used by Krider *et al*. [19] for the calibration of their measurement of lightning energy was dissipated in the hot return-stroke channel, the bulk of the input energy being dissipated in the "plasma ahead of the advancing secondary streamer" during the preceding leader processes. Cooray [69], from electrostatic considerations, estimated that two-thirds of the subsequent-stroke input energy is dissipated in the dart-leader stage and one-third in the return-stroke stage, whereas for first strokes roughly one-third of the input energy is dissipated in the stepped-leader stage and two-thirds in the return-stroke stage. If an appreciable portion of the input energy is dissipated during the leader process, Krider *et al*.'s [19] energy estimate cannot be compared directly with model predictions which only consider the return-stroke process. On the other hand, lightning input energy of the order of 10^5 J/m appears to be consistent with the thunder theory of Few [70], [71], although this theory itself remains a subject of debate. Also, this value of lightning energy is comparable to that inferred from the electrostatic model of the thundercloud (e.g., Uman [20] and Table I), although a significant fraction of electrostatic energy available to lightning is likely dissipated by processes other than the return stroke, including the in-cloud discharge processes that *effectively* serve to collect charges from isolated hydrometers in volumes measured in cubic kilometers and to transport those charges into the developing leader channel. Additional experimental data are needed to resolve the two orders of magnitude uncertainty in the value of lightning input energy.

B. Electromagnetic Models

For the electromagnetic models, as well as for the distributed-circuit and "engineering" models, the most appropriate test of model validity would appear to be a comparison of the model-predicted electromagnetic fields to the measured fields. Measured electric and magnetic fields due to natural lightning at 1–200 km presented by Lin *et al*. [72] and electric fields due to triggered lightning at 30–110 m published by Uman *et al*. [73], [74] and Rakov *et al*. [75] are presently the most useful data for such an evaluation. These are reproduced in Fig. 10(a) and (b), respectively.

Podgorsky and Landt [22] do not give any model-predicted fields. Moini *et al*. [23] have demonstrated fairly good agreement between the model-predicted and typical measured electric fields at distances ranging from tens of meters to tens of kilometers. At 100 km, their model does not predict a field zero-crossing within 200 μs or so and, hence, is inconsistent with published measured fields at this distance [see Fig. 10(a)]. The significance of the zero-crossing time as a criterion of model validity is discussed in Section VI-D.

C. Distributed-Circuit Models

Electromagnetic fields calculated by Takagi and Takeuti [35, figs. 12, 13] and Price and Pierce [33, fig. 4], who used linear distributed-circuit models, and by Mattos and Christopoulos

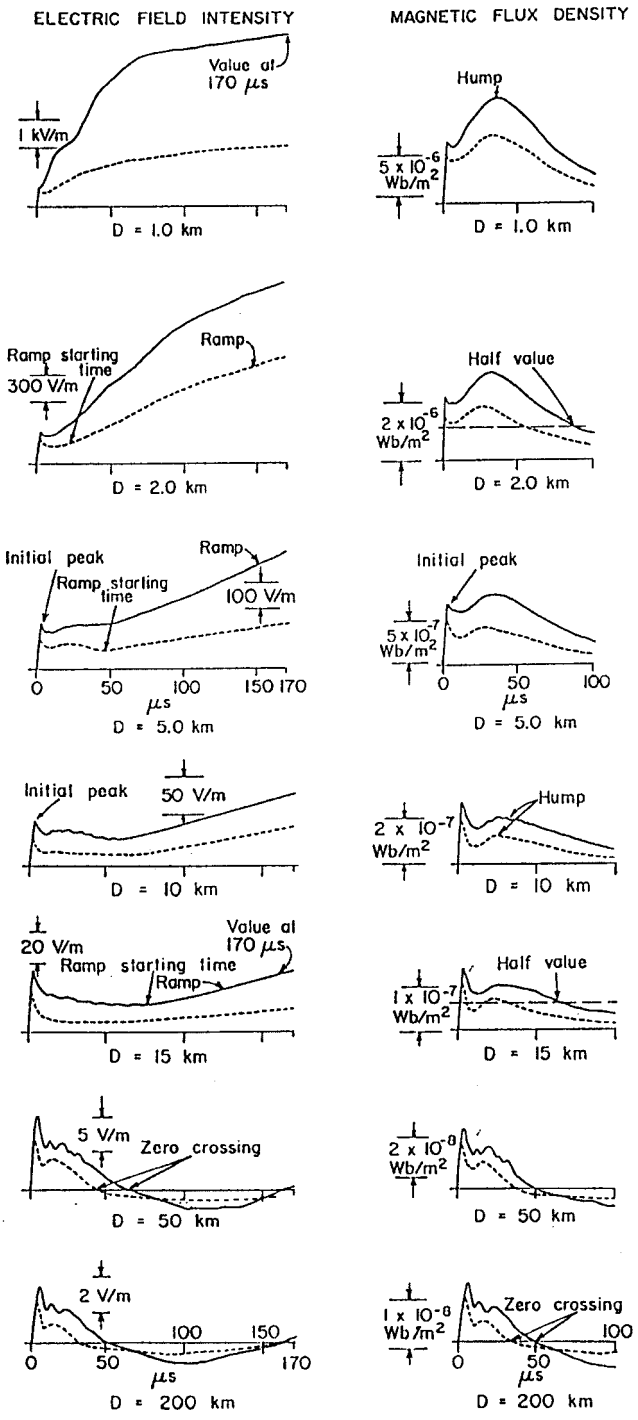

(a)

Fig. 10. (a) Typical vertical electric field intensity (left column) and horizontal magnetic flux density (right column) waveforms for first (solid line) and subsequent (dashed line) return strokes at distances of 1, 2, 5, 10, 15, 50, and 200 km. The following characteristic features of the waveforms are identified for electric field, initial peak, ramp starting time, ramp, 170-μs value, and zero crossing; for magnetic field—initial peak, hump, half-value. Adapted from Lin *et al.* [72].

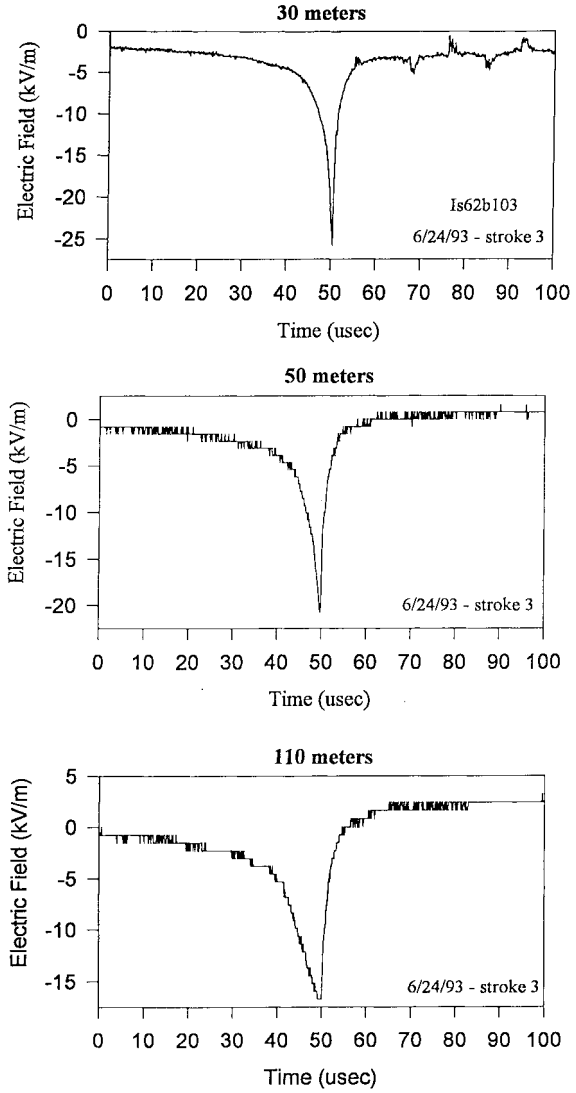

Fig. 10. *(Continued.)* (b) Typical vertical electric field intensity waveforms for dart leader/return stroke sequences in triggered lightning at 30, 50, and 110 m. The initial downward-going portion of the waveform is due to the dart leader. The return stroke produces the upward-going portion (beginning at 50 μs) of the waveform. Note a characteristic flattening of the rising return-stroke field within 15 μs or so. Adapted from Uman *et al.* [73].

[40, figs. 7–9] and Baker [42, figs. 3, 6], who used nonlinear distributed-circuit models, are largely inconsistent with typical measured fields [see Fig. 10(a)], although Mattos and Christopoulos [40] claim the opposite. Other authors do not present model-predicted electromagnetic fields, leaving their models unverified by the most readily available experimental data.

D. "Engineering" Models

Two primary approaches to model validation have been used. The first approach involves using a *typical* channel-base current waveform and a *typical* return-stroke propagation speed as model inputs and then comparing the model-predicted electromagnetic fields with *typically* observed fields. The second approach involves using the channel-base current waveform and the propagation speed measured for the same *individual* event and comparing computed fields with measured fields for that same *specific* event. The second approach is able to provide a more definitive answer regarding model validity, but it is feasible only in the case of triggered-lightning

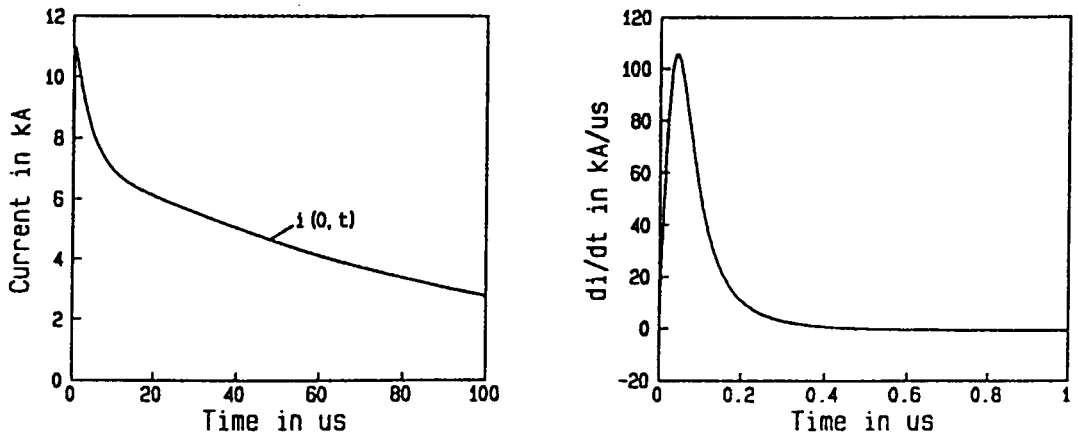

(a) (b)

Fig. 11. (a) Specified current at ground level. (b) Current derivative used by Nucci *et al.* [57] (also by Rakov and Dulzon [45] and by Thottappillil *et al.* [43]) for validation of return-stroke models by the "typical return-stroke" approach.

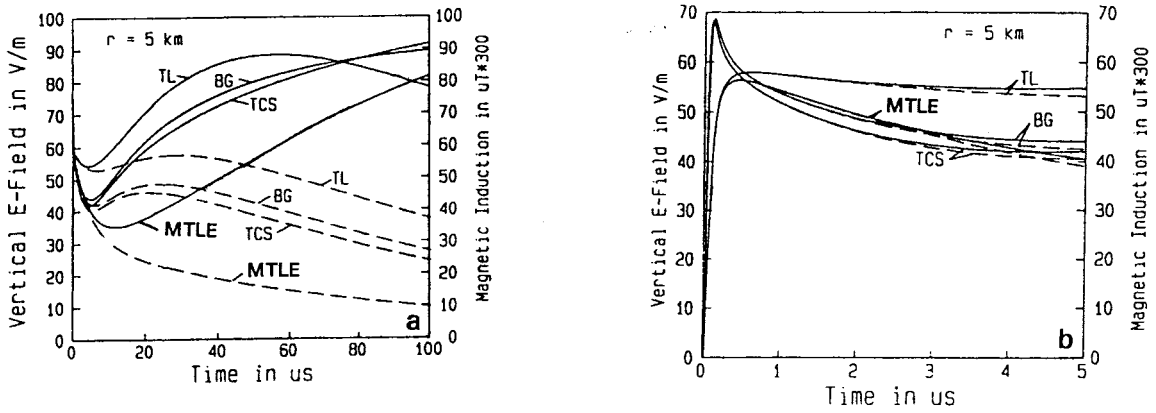

(a) (b)

Fig. 12. Calculated electric (left scaling, solid lines) and magnetic (right scaling, dashed lines) fields for four models at a distance $r = 5$ km for (a) 100 μs and (b) the first 5 μs. Adapted from Nucci *et al.* [57].

return strokes or natural lightning strikes to tall towers where channel-base current can be measured. In the field calculations, the channel is generally assumed to be straight and vertical with its origin at ground $(z' = 0)$, conditions which are expected to be valid for subsequent strokes, but potentially not for first strokes. The channel length is usually not specified unless it is an inherent feature of the model, as is the case for the MTLL model (e.g., Rakov and Dulzon [47]). As a result, the model-predicted fields and associated model validation may not be meaningful after 25–75 μs, the typical time required for the return-stroke front to traverse the distance from ground to the cloud charge source.

1) "Typical Return-Stroke" Approach: This approach has been adopted by Nucci *et al.* [57], Rakov and Dulzon [45], and Thottappillil *et al.* [43]. Nucci *et al.* [57] identified four characteristic features in the fields at 1 to 200 km measured by Lin *et al.* [72] [see Fig. 10(a)] and used those features as a benchmark for their validation of the TL, MTLE, BG, and TCS models (also of the MULS model, not considered here). The characteristic features include: 1) a sharp initial peak that varies approximately as the inverse distance beyond a kilometer or so in both electric and magnetic fields; 2) a slow ramp following the initial peak and lasting in excess of 100 μs for electric fields measured within a few tens of kilometers; 3) a hump following the initial peak in magnetic fields within a few tens of kilometers, the maximum of which occurs between 10 and 40 μs; and 4) a zero crossing within tens of microseconds of the initial peak in both electric and magnetic fields at 50 to 200 km. For the current (see Fig. 11) and other model characteristics assumed by Nucci *et al.* [57], feature 1) is reproduced by all the models examined, feature 2) by all the models except for the TL model, feature 3) by the BG, TL and TCS models but not by the MTLE model, and feature 4) only by the MTLE model but not by the BG, TL, and TCS models, as illustrated in Figs. 12 and 13. Diendorfer and Uman [53] showed that the DU model reproduces features 1), 2), and 3) and Thottappillil *et al.* [76] demonstrated that a relatively insignificant change in the channel-base current waveform (well within the range of typical waveforms) allows the reproduction of feature 4), the zero crossing, by the TCS and DU models. Rakov and Dulzon [45] showed that the MTLL model reproduces features

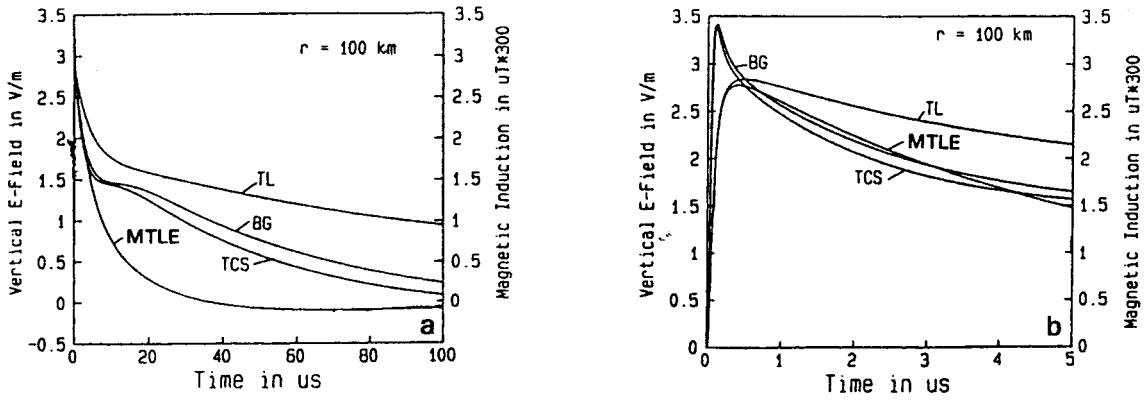

(a) (b)

Fig. 13. Calculated electric (left scaling) and magnetic (right scaling) fields for four models at a distance $r = 100$ km for (a) 100 μs and (b) the first 5 μs. Adapted from Nucci *et al.* [57].

1), 2), and 4). The observed sensitivity of the distant field waveforms predicted by the TCS and DU models to the variations in the channel-base current waveform has important implications for the validation of models. Indeed, since appreciable variation in the current waveform is a well documented fact (e.g., Uman [20, table 7.2]), the relatively narrow range of observed zero-crossing times (e.g., Uman [20, table 7.1]) appears inconsistent with the TCS and DU models. On the other hand, the experimental field data might be biased toward earlier zero-crossing times and more pronounced opposite polarity overshoots due to the following two reasons. First, the oscilloscope sweep of 200 μs was insufficient to measure relatively long zero crossing times. Second, the initial rising portion of the waveform was apparently not always completely recorded (the first recorded point on the waveform was 2.5 μs prior to the time of trigger) and, as a result, the zero field level apparently was sometimes set at a point on the waveform that was higher than the actual zero field level. Nucci *et al.* [57] conclude from their study that all the models evaluated by them using measured fields at distances ranging from 1 to 200 km predict reasonable fields for the first 5–10 μs, and all models except the TL model do so for the first 100 μs.

Thottappillil *et al.* [43] noted that measured electric fields at tens to hundreds of meters from triggered lightning (e.g., Uman *et al.* [73], [74]; Rakov *et al.* [75]) exhibit a characteristic flattening within 15 μs or so, as seen in Fig. 10(b). Electric fields predicted at 50 m by the BG, TL, MTLL, TCS, MTLE, and DU models are shown in Fig. 14, taken from Thottappillil *et al.* [43]. As follows from this figure, the BG, MTLL, TCS, and DU models, but not the TL and MTLE models, are consistent with the measured fields presented in Fig. 10(b). Additionally, the MTLE model is inconsistent with the observed ratio of leader-to-return-stroke electric field change at far ranges, as illustrated in Table V taken from [43]. As seen in Table V, at 20 to 50 km the measured ratio is near unity [77] (in support of the BG, MTLL, TCS, and DU models), whereas the MTLE model predicts a value near three.

2) "Specific Return-Stroke" Approach: This approach has been adopted by Thottappillil and Uman [78] who compared the TL, TCS, MTLE, DU, and MDU models. They used 18

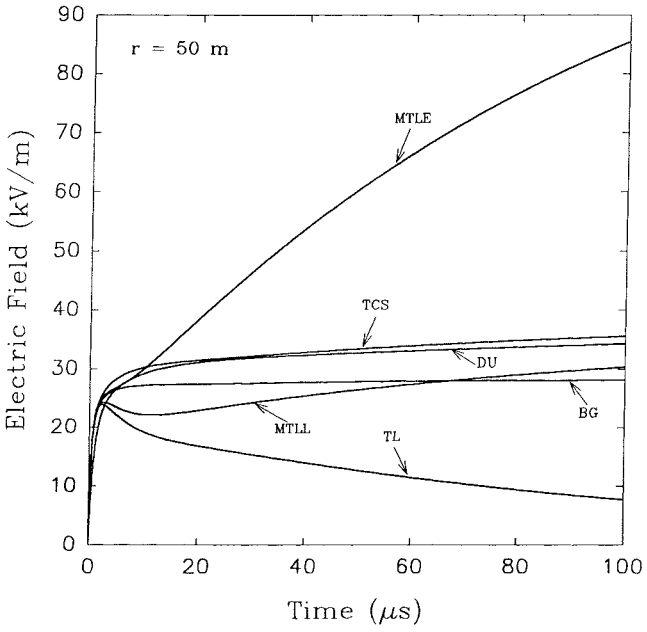

Fig. 14. Calculated electric fields for six return-stroke models at a distance $r = 50$ m, to be compared with typical measured return-stroke field at 50 m presented in Fig. 10(b). Note that only the upward-going portion of the waveforms shown in Fig. 10(b) is due to the return stroke, the downward-going portion being due to the preceding dart leader. Adapted from Thottappillil *et al.* [43].

sets of three simultaneously measured features of triggered-lightning return strokes: channel-base current, return-stroke propagation speed, and electric field at about 5 km from the channel base, the data previously used by Willett *et al.* [79] for their analysis of the TL model. Examples of the comparisons for three strokes characterized by somewhat different rising portions of the channel-base current, shown in Fig. 15, are given in Figs. 16–18 for the TL, TCS, MTLE, and DU models. It has been found that the TL, MTLE, and DU models each predict the measured initial electric field peaks within an error whose mean absolute value is about 20%, while the TCS model has a mean absolute error about 40%.

3) Summary: The overall results of the validation of the "engineering" models can be summarized as follows.

TABLE V
RATIO OF LEADER-TO-RETURN-STROKE ELECTRIC FIELD AS A FUNCTION OF DISTANCE AS PREDICTED BY FIVE RETURN-STROKE MODELS VERSUS OBSERVATIONS. ADAPTED FROM THOTTAPPILLIL *ET AL.* [43]

Return-Stroke Model	Distance, km					
	0.05	1	5	20	50	100
MTLL	-0.99	-0.85	- 0.14	+ 0.81	+ 0.97	+ 0.99
MTLE	-1.0	-0.92	+ 0.14	+ 2.6	+ 3.0	+ 3.1
BG	-1.0	-0.87	- 0.09	+ 1.1	+ 1.2	+ 1.3
TCS	-1.0	-0.88	- 0.08	+ 1.1	+ 1.3	+ 1.4
DU	-1.0	-0.88	- 0.08	+ 1.1	+ 1.3	+ 1.4
Experimental Mean Values	-1.0(6)[a]	-0.81(6)[b]	- 0.17(12)[c]		+ 0.8(97)[d]	-

In the model calculations, only the deposited charge density component is used. For the MTLL and MTLE models the deposited charge density component is calculated at $t = 1$ ms. $H = 7.5$ km; $\lambda = 2$ km; $\tau_D = 0.1$ μs; current at the channel base is the same as that adopted by *Nucci et al.* [57, Figure 4a]. In the last row, the numbers in the parentheses indicate the sample sizes of the experimental data.

[a] *Rakov et al.* [75, Table 1]; triggered-lightning strokes.
[b] *Beasley et al.* [77, Figure 23b]; distance range from 1 to 2 km; first strokes in natural lightning.
[c] *Rakov et al.* [82, Figure 3a]; distance range from 4 to 6 km; first strokes in natural lightning.
[d] *Beasley et al.* [77, Figure 23d]; first strokes in natural lightning.

1) The relation between the initial field peak and the initial current peak is reasonably well predicted by the TL, MTLL, MTLE, and DU models.
2) Electric fields at tens of meters from the channel after the first 10 to 15 μs are reasonably reproduced by the MTLL, BG, TCS and DU model, but not by the TL and MTLE models.
3) From the standpoint of the overall field waveforms at 5 km (the only distance at which the "specific return-stroke" model validation approach has been used) all the models should be considered less than adequate.

Based on the entirety of the validation results and mathematical simplicity, we rank the "engineering" models in the following descending order: MTLL, DU, MTLE, TSC, BG, and TL. However, the TL model is recommended for the estimation of the initial field peak from the current peak or conversely the current peak from the field peak, since it is the mathematically simplest model with a predicted peak field/peak current relation that is equally or more accurate than that of the more mathematically complex models.

VII. FURTHER TOPICS IN RETURN-STROKE MODELING

In this section, we discuss several potentially important aspects of return-stroke modeling that have either been ignored to keep the modeling straightforward or have simply not been recognized. Only models of the "engineering," distributed-circuit, and electromagnetic types are considered here.

A. Treatment of the Upper In-Cloud Portion of the Channel

It is the common view (e.g., Lin *et al.* [80]) that subsequent return strokes are easier to model than first strokes. First strokes are commonly branched, may involve an upward connecting discharge from ground of appreciable length (perhaps many tens of meters) and typically exhibit a significant variation of propagation speed along the channel. This view is correct as long as the lightning channel is predominantly vertical, a condition that is less likely to be satisfied for subsequent strokes than for first strokes after the return stroke reaches cloud charge height, typically after 25–75 μs assuming that the return-stroke front propagation speed in the cloud is approximately the same as that below the cloud base. Subsequent strokes are expected (Krehbiel *et al.* [81], Rakov *et al.* [82]) to follow predominantly horizontal paths in the cloud charge region. Additionally, none of the "engineering" models except the MTLL model specifies boundary conditions at the channel top. A reflection should be produced when the return-stroke front encounters an impedance discontinuity at the channel top. Some indirect evidence of the channel top reflection apparently comes from the VHF interferometric studies of Shao *et al.* [83, p. 2759] who observed VHF bursts, indicative of breakdown, at the preceding-leader starting point when the return stroke arrived there. Further, the channel-base current waveshape for the first strokes in altitude-triggered lightning appears to be significantly modified by the reflection from the upper end of the channel at 1 km or so (Rakov *et al.* [75]). Various boundary conditions at the channel top have been considered in the distributed-circuit models, including an open circuit (Strawe [12], Baker [42]), a capacitor or an L-C transmission line (Takagi and Takeuti [35]), and an R-C network (Mattos and Christopoulos [39], [40]). When only the first few microseconds of the field waveforms are of interest, which is often the case in EMC applications since that is when the peak field and peak field derivatives occur, the treatment of the channel top becomes unimportant.

B. Boundary Conditions at Ground

In the transmission-line-type "engineering" models, the boundary conditions at ground are determined by the specified

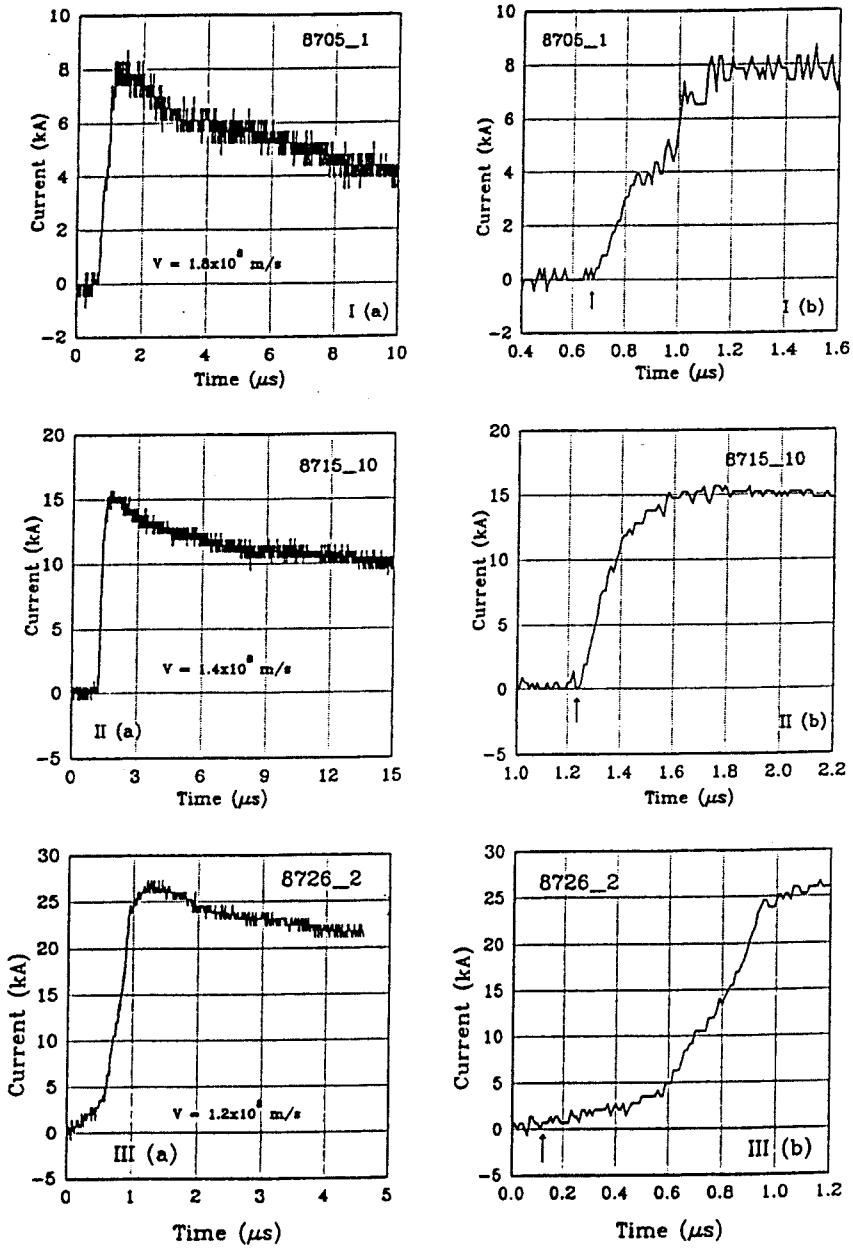

Fig. 15. (a) Total available current waveform. (b) The wave front on an expanded time scale at the base of the channel for three different triggered-lightning return strokes 8705_1 (I) 8715_10 (II) and 8726_2 (III) used by Thottappillil and Uman [78] for validation of return-stroke models by the "specific return-stroke" approach. Also given for each stroke is the measured return-stroke speed. Adapted from Thottappillil and Uman [78].

channel-base current; that is, by a current source at the channel bottom. In the TCS and DU models, those models which assume that the return-stroke current is generated at the upward-moving front and propagates toward ground, it is usually implied that the channel is terminated at ground in its characteristic impedance so that the current reflection coefficient at ground is equal to zero. This implication is invalid for the case of a lightning strike to a well-grounded object where an appreciable reflection from ground is expected. Extensions of the TCS model to include reflection at ground and at the upward moving front are considered in Section V. In the distributed-circuit return-stroke models, the boundary conditions at ground are specified explicitly, with a terminating resistor (typically tens to hundreds of ohms) being used to simulate earth resistance.

Some "engineering" models have been extended to include a grounded strike object modeled as an ideal transmission line that supports the propagation of waves at the speed of light without attenuation or distortion (e.g., Diendorfer and Uman [53]; Guerrieri *et al*. [84]; Rachidi *et al*. [85]). Such an extension results in a second current wave front that propagates from the top of the object toward ground at the speed of light and either produces no reflection on its arrival there implying that the ground impedance is equal to the surge impedance of the object (e.g., Diendorfer and Uman [53]) or is allowed to bounce between the top and bottom ends of the object and, in

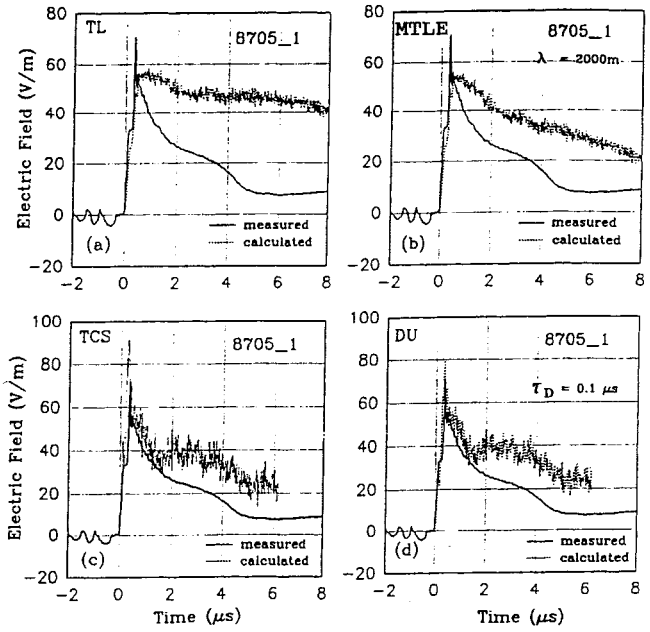

Fig. 16. Comparison of calculated vertical electric fields from models (a) TL, (b) MTLE, (c) TCS, and (d) DU with the measured field at 5.16 km for return stroke 8705_1. The measured current at the channel base and the measured return-stroke speed are given in Fig. 15, panels Ia and Ib. Adapted from Thottappillil and Uman [78].

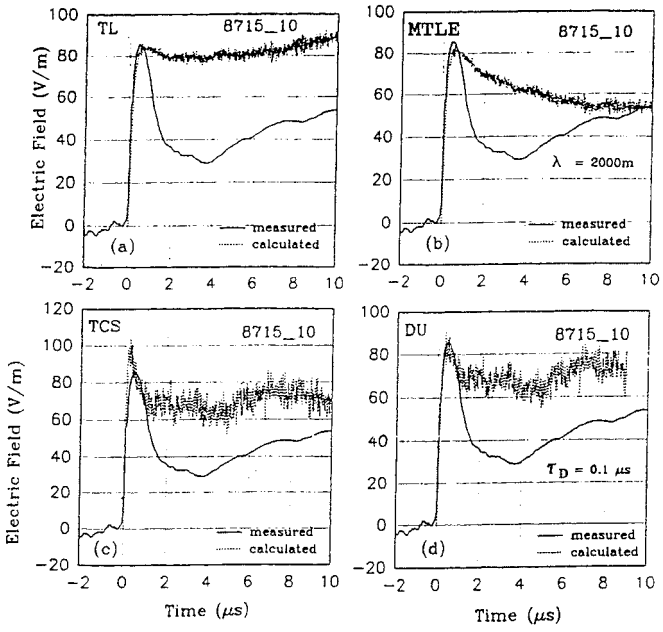

Fig. 17. Comparison of calculated vertical electric fields from models (a) TL, (b) MTLE, (c) TCS, and (d) DU with the measured field at 5.16 km for return stroke 8715_10. The measured current at the channel base and the measured return-stroke speed are given in Fig. 15, panels IIa and IIb. Adapted from Thottappillil and Uman [78].

general, produce transmitted waves at either end (e.g., Guerrieri *et al*. [84], Rachidi *et al*. [85]). The electromagnetic model developed by Podgorski and Landt [22] includes the simulated strike object, the 553-m-high CN (Canadian National) tower in Toronto, represented by a 3-D wire structure. The bouncing

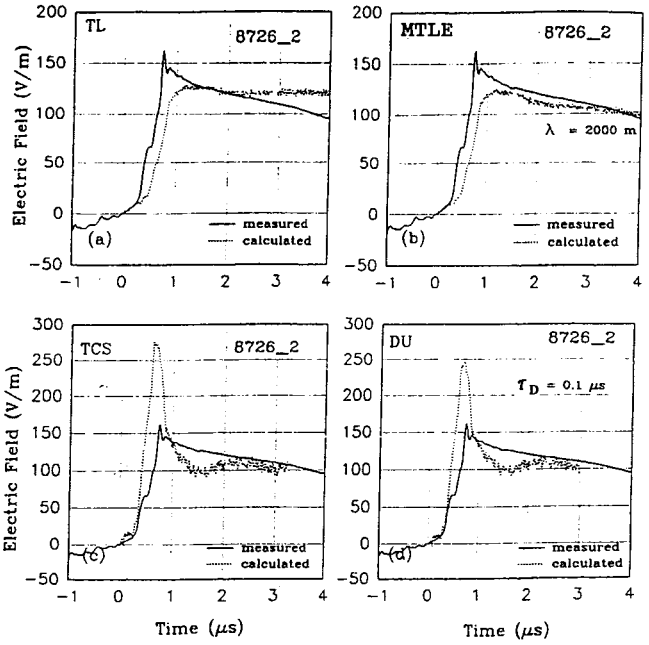

Fig. 18. Comparison of calculated vertical electric fields from models (a) TL, (b) MTLE, (c) TCS, and (d) DU with the measured field at 5.16 km for return stroke 8726_2. The measured current at the channel base and the measured return-stroke speed are given in Fig. 15, panels IIIa and IIIb. Adapted from Thottappillil and Uman [78].

waves on the strike object serve to carry the information on the conditions at the bottom of the object (grounding impedance) to the top of the object. In the simple example of a *nonideal* current source attached to the top of the object and generating a step-function current wave, the magnitude of the wave injected into the object depends on the characteristic impedance of the object. Specifically, the total source current divides between the source impedance and the object inversely to that source impedance and the surge impedance of the object. However, after a sufficiently long period of time, current magnitude at any point on the object will be equal to the magnitude of current that would be injected directly into the grounding impedance of the object from the same current source in the absence of the object. Note that the above example applies only to a step-function current wave, the current distribution along the object being more complex for the case of an impulsive current waveform characteristic of the lightning return stroke. If the lightning current wave round-trip time on the strike object is appreciably longer than the risetime of current measured at the top of the object, the reflected-current peak separates from the incident-current peak in the overall current waveform in the upper part of the object. The presence of a vertically extended strike object may substantially increase the initial peak electric and magnetic fields and the electric and magnetic field derivatives at early times, compared to the case of the return stroke being initiated at ground level. Note that when the shortest significant wavelength in the lightning current is much longer than the height of the strike object, there is no need to consider the distributed-circuit behavior of such an object. For example, if the minimum significant wavelength is 300 m (1 MHz), objects whose heights are about 30 m or

less (about 3 m for a minimum significant wavelength of 30 m) may be considered as lumped, in most cases as a short circuit between the lightning channel base and ground.

C. Return-Stroke Front Speed at Early Times

Baum [31] has argued that at the instant of return-stroke initiation the geometry of the bottom some tens of meters of the leader channel is an inverted circular cone because the corona closer to ground has not had enough time for its full development. Propagation speeds of radial corona streamers from conductors subjected to negative high voltage in the laboratory were reported to be about 10^5 m/s (0.1 m/μs) (Cooray [58]) so that some microseconds are required for the development of a corona sheath with a radius of the order of meters. For stepped leaders, the average downward propagation speed is also of the order of 10^5 m/s so that there is a relatively short delay in the corona-sheath formation as a stepped leader moves toward ground, although it is not clear what is occurring during the attachment process. For dart leaders, the downward propagation speeds (10^7 m/s) are about two orders of magnitude higher than the radial-streamer speed (if it still applies) so that the delay may be appreciable. The charge density in Baum's [31] model is zero at ground and increases linearly with height. The conical model of the bottom part of the channel predicts an initial return-stroke speed of nearly c, the speed of light, because both the longitudinal channel current and channel charge near ground are confined in a volume of approximately the same radial dimension. The speed is predicted by Baum [31] to decrease in some hundreds of nanoseconds to approximately $c/3$ when the return-stroke front reaches a height of the order of tens of meters where the corona sheath is fully developed and the channel geometry is cylindrical; that is, where the radii of the current-carrying channel core and the charge-containing corona sheath appreciably differ from each other. However, return-stroke speed versus height profiles measured within 400 m of ground for two triggered-lightning strokes by Wang *et al*. [86] indicate an initial upward speed of the order of one-third to one-half the speed of light with apparently no systematic variation in the bottom 100 m or so of the channel. Wang *et al*. [86] used the digital optical imaging system ALPS (Yokoyama *et al*. [87]) with 100 ns time resolution. The spatial resolution of their measurements was about 25 m.

Some researchers have attempted to estimate return-stroke speed using (4) and (5). Such estimates are necessarily model dependent and often are difficult to interpret, as discussed below. Leteinturier *et al*. [88] estimated the return-stroke speed using: 1) measured peak time-derivatives of the channel-base current; 2) measured peak time derivatives of the electric field at 50 m; and 3) (5). They reported the speed values to be on average near c, with 14 out of 40 values being greater than the speed of light. Baum [31] invoked these model-dependent speed estimates in support of his theoretical prediction that the initial return-stroke speed is nearly equal to the speed of light. On the other hand, similar estimates of speed using peak electric field derivatives measured at about 5 km give a mean value of approximately two-thirds of c (Willett *et al*. [79]). Further, the use of: 1) measured channel-base current peak; 2) measured electric field peak at about 5 km; and 3) (4) leads to a mean return-stroke speed of about one-half of c, consistent with corresponding optical speed measurements over the bottom 400–600 m of the channel (Willett *et al*. [79]). It is possible that since the peak derivative precedes the peak of electric field or current, speed estimates using (5); that is, using the peak time derivatives of electric field and current are representative of a somewhat lower channel section than those based on (4); that is, on peak electric field and peak current. On the other hand, this conjecture implies a very rapid speed decay within the bottom 100 m or so while, as it is stated above, the measurements of Wang *et al*. [86] do not appear to indicate a systematic speed variation near the bottom of the channel. Additionally, such a rapid speed decay would probably render (4) and (5), derived assuming a constant v, invalid. Another possible explanation for the discrepancy between the speeds inferred from (5) using the 50-m and 5-km data is the contribution of the induction and electrostatic field components at 50 m to the total electric field derivative peak, this contribution not being accounted for in (5), which is derived for the radiation field component only (Cooray [89]; Leteinturier *et al*. [88]). The discrepancy between the three return-stroke speed estimates made using (4) and (5), near c, $2c/3$, and $c/2$ discussed above, remains unresolved and may indeed be due to the inadequacy of the TL model from which (4) and (5) are derived. Additional discussion of these speed estimates is found in Section VII-D.

A different return-stroke speed profile is suggested by Gorin [29]. According to his distributed-circuit model for the case of a first stroke, the speed initially increases to its maximum over a channel length of the order of some hundreds of meters and decreases thereafter. The initial speed increase in Gorin's model is associated with the so-called break-through phase (also called the final jump or switch-closing phase) possibly responsible for the formation of the initial rising portion of the return-stroke current pulse (see also, Rakov and Dulzon [45], Rakov *et al*. [90]). Srivastava [91] proposed, based on the experimental data published by Schonland [92], a bi-exponential expression for the first return-stroke speed as a function of time according to which the speed rises from zero to its peak and falls off afterwards. More experimental data on the attachment process and on the early stages of the return-stroke process are needed to deduce the typical first and subsequent return-stroke speed profiles near ground.

D. Initial Bidirectional Extension of the Return-Stroke Channel

The initial bidirectional extension of the return-stroke channel was hypothesized by Wagner and Hileman [93], Uman *et al*. [94], Willett *et al*. [95], and Leteinturier *et al*. [88]. The first direct experimental evidence of such extension is presented by Wang *et al*. [96]. Using the ALPS with 3.6-m spatial and 100-ns time resolution, they observed an upward connecting discharge in one triggered-lightning stroke and inferred the existence of such a discharge in another stroke. In both events, the return stroke was initially a bidirectional process with the upward and downward moving waves originating at 7–11 m above the strike object in the event with an imaged

upward connecting discharge and 4–7 m in the event with no imaged upward connecting discharge. Both upward and downward moving wavefronts necessarily contribute to the remote electric and magnetic fields, while current measured at the channel base is thought to be associated only with the downward wave and its reflection at ground. Equations (4) and (5) derived for a single wave are in general invalid during the time of the initial bidirectional extension of the return-stroke channel. The electromagnetic model of Podgorski and Landt [22] and the distributed-circuit model of Strawe [12] include an upward connecting discharge channel which facilitates the initial bidirectional development of the return-stroke process.

E. Relation Between Leader and Return-Stroke Models

Usually, the lightning leader and the lightning return stroke are each modeled independently, the implicit assumption being that the leader process ends or becomes negligible when the return stroke begins. However, the return stroke operates on the charge deposited onto the channel by the preceding leader and, therefore, these two lightning processes should be strongly coupled. Indeed, Rubinstein *et al*. [97] and Rakov *et al*. [75] inferred from triggered-lightning experiments that the return-stroke current peak at the channel base is largely determined by the dart-leader charge density within the bottom tens to hundreds of meters of the channel, a height consistent with typical return-stroke front speed and typical channel-base current risetime, the product of these two quantities giving the height of the return-stroke front at the time when the channel-base current peak is formed. Formulation of the return-stroke model in terms of charge density (Thottappillil *et al*. [43]) (see Tables III and IV) provides a direct link to the dart-leader model, assuming that all leader charge is neutralized by the return stroke and that the latter does not deposit any additional charge on the channel. Further, Rakov [28] has suggested that the subsequent return stroke could be quite possibly viewed as a ground "reflection" of the dart leader.

VIII. Calculation of Lightning Return Stroke Electric and Magnetic Fields

As follows from our classification of models given in the Introduction, we define a lightning return-stroke model of electromagnetic, distributed-circuit, or "engineering" type as an equation or set of equations that allows one to determine the return-stroke current as a function of a spatial (vertical) coordinate and time. This current is the source that is used to compute the lightning electric and magnetic fields. The gas dynamic models are an exception being considered here primarily because they can be used to find the R needed for the electromagnetic and distributed-circuit models. Thus, the calculation of electromagnetic fields, according to our definition, is an application rather than part of the model, although some authors (e.g., Willett *et al*. [95], Leteinturier *et al*. [88], Le Vine and Willett [98]) use the term "return-stroke model" to denote a field/current relation such as (4). When it comes to model validation, the latter approach does not distinguish between the model of the source and the field computing model. For example, (4), in addition to the model

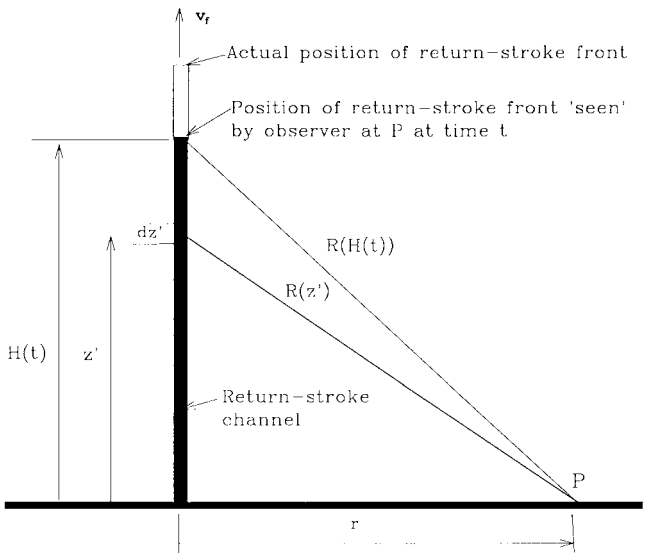

Fig. 19. Geometry used in deriving (6) and (7) for electric and magnetic fields, respectively, at a point P on earth (assumed to be perfectly conducting) a horizontal distance r from the vertical lightning return-stroke channel extending upward with speed v_f. Adapted from Thottappillil *et al*. [43].

description of the source, involves the assumptions that the field is pure radiation, the ground is perfectly conducting, and the field point is far enough to consider all contributing source points as essentially equidistant from that field point. Note that once the source is specified, fields can always be computed without approximation other than those involved in the computational process.

A. Electric and Magnetic Field Equations

Most general equations for computing the vertical electric field E_z and azimuthal magnetic field B_ϕ due to an upward-moving return stroke for the case of a field point P on ground (see Fig. 19) are given by Thottappillil *et al*. [43] and reproduced as follows:

$$\begin{aligned} E_z(r,t) &= \frac{1}{2\pi\varepsilon_0}\int_0^{H(t)}\left[\frac{2z'^2-r^2}{R^5(z')}\int_{\frac{z'}{v_f}+\frac{R(z')}{c}}^{t} I\left(z',\tau-\frac{R(z')}{c}\right)d\tau \right. \\ &\quad + \frac{2z'^2-r^2}{cR^4(z')}I\left(z',t-\frac{R(z')}{c}\right) \\ &\quad \left. - \frac{r^2}{c^2R^3(z')}\frac{\partial I(z',t-R(z')/c)}{\partial t}\right]dz' \\ &\quad - \frac{1}{2\pi\varepsilon_0}\frac{r^2}{c^2R^3(H(t))}I\left(H(t),\frac{H(t)}{v_f}\right)\frac{dH(t)}{dt} \end{aligned} \tag{6}$$

$$\begin{aligned} B_\phi(r,t) &= \frac{\mu_0}{2\pi}\int_0^{H(t)}\left[\frac{r}{R^3(z')}I\left(z',t-\frac{R(z')}{c}\right)\right. \\ &\quad \left. + \frac{r}{cR^2(z')}\frac{\partial I(z',t-R(z')/c)}{\partial t}\right]dz' \\ &\quad + \frac{\mu_0}{2\pi}\frac{r}{cR^2(H(t))}I\left(H(t),\frac{H(t)}{v_f}\right)\frac{dH(t)}{dt} \end{aligned} \tag{7}$$

where $H(t)$ is the height of the front as "seen" by the observer at time t (see Fig. 19). This height can be found from the following equation:

$$t = \frac{H(t)}{v_f} + \frac{R(H(t))}{c}. \tag{8}$$

Thottappillil *et al*. [43] also give the equivalent electric and magnetic field equations in terms of channel charge density ρ instead of channel current I. The first three terms in (6) and the first two terms in (7) describe the field due to source points below the upward moving front, while the last terms in these equations account for possible discontinuity at the moving front. A discontinuity at the upward moving front is an inherent feature of the BG and TCS models, even when current at the channel base starts from zero (see Fig. 8). The transmission-line-type models may include a discontinuity at the front if the channel-base current starts from a nonzero value. The DU model does not allow a current discontinuity either at the upward-moving front or at the channel base. The front discontinuity produces only a radiation field component, no electrostatic or induction field components.

Note that (6) and (7), when used for numerical computations, take proper account of retardation effects, as shown by Thottappillil *et al*. [99] and, therefore, do not require any correction such as via the so-called F factor considered by Rubinstein and Uman [100], [101], Le Vine and Willett [98], and Krider [102]. These equations are suitable for computing fields at ground using the electromagnetic, distributed-circuit, or "engineering" return-stroke models.

The computation of lightning return stroke electric and magnetic fields for the case of an observation point elevated up to 10 km above ground has been considered by Master *et al*. [3].

B. Channel-Base Current Equation

In the case of the "engineering" models assuming a vertical lightning channel and a perfectly conducting ground, the information on the source required for computing fields usually includes: 1) the channel base current (either measured or assumed based on typical measurements) and 2) the upward return-stroke front speed, typically assumed to be constant in a range from 1×10^8 to 2×10^8 m/s (see Rakov *et al*. [90] for a summary of measured speeds). The typical subsequent-stroke current waveform at the channel base is often approximated by an expression containing the so-called Heidler function [50]

$$I(0,t) = \frac{I_0}{\eta} \frac{(t/\tau_1)^n}{(t/\tau_1)^n + 1} e^{-t/\tau_2} \tag{9}$$

where I_0, η, τ_1, n, and τ_2 are constants. This function allows one to change conveniently the current peak, maximum current derivative, and associated electrical charge transfer nearly independently by changing I_0, τ_1, and τ_2, respectively. Equation (9) reproduces the observed concave rising portion of a typical current waveform as opposed to the once more commonly used double-exponential function, introduced by Bruce and Golde [49], which is characterized by an unrealistic convex wavefront with a maximum current derivative at $t = 0$. A current equation capable of reproducing a concave, convex, or linear wavefront was used in [47]. Sometimes a sum of two Heidler functions with different parameters is used to approximate the desired current waveshape. Diendorfer and Uman [53], for example, described the subsequent-stroke current waveform at the channel base as the sum of two functions given by (9). The first function is characterized by $I_0 = 13$ kA, $\eta = 0.73$, $\tau_1 = 0.15$ μs, $n = 2$, and $\tau_2 = 3.0$ μs, and the second one by $I_0 = 7$ kA, $\eta = 0.64$, $\tau_1 = 5$ μs, and $\tau_2 = 50$ μs. The resultant current peak is 14 kA and the maximum current rate of rise is 75 kA/μs. The current waveform used by Nucci *et al*. [57] and reproduced in Fig. 11 is the sum of a Heidler function and a double-exponential function.

C. Channel Tortuosity and Branches

In most computations of fields due to the return stroke, the return-stroke channel is assumed to be straight, while it is known to be tortuous on scales ranging from less than 1 m to over 1 km (e.g., Salanave [103], Hill [104], [105]). The "microscale" tortuosity, including geometric features with lengths of the order of 10 cm or less, of triggered-lightning channels has been examined in detail by Idone [106]. Le Vine and Willett [107] present experimental evidence suggesting that the channel geometry is a factor in determining the fine structure observed during the first 10 μs of the electric fields produced by return strokes in both natural and triggered lightning. In the case of natural lightning, only subsequent strokes were considered. The effects of channel tortuosity on return stroke radiation fields have been studied theoretically using a piecewise linear representation of the lightning channel and simple return-stroke models by Hill [105], Le Vine and Meneghini, [108], [109] Le Vine *et al*. [110], Le Vine and Kao [111], Gardner [112], Cooray and Orville [113], and Vecchi *et al*. [114]. The lengths of individual linear channel segments were typically of some tens to some hundreds of meters. In general, the effect of tortuosity was to introduce fine structure into the time-domain radiation field waveform and consequently to increase the higher frequency content, above 100 kHz or so according to Le Vine and Meneghini [108], of the waveform. At each kink; that is, point at which the linear segments joint, there is a change in the direction of the propagation of the current wave and such changes introduce rapid variations in the radiation field. The amount of fine structure due to channel tortuosity depends on the current waveshape. Significant variations in the radiation field are produced when the risetime of the current waveform is smaller than the time required for the current wave to propagate between kinks (Le Vine and Kao [111], Cooray and Orville [113]). When the risetime is significantly larger than the propagation time between kinks, then more than one kink contributes to the radiation field during the rising portion of the current wave, and, as a result, an averaging (smoothing) effect of the overall field occurs. Cooray and Orville [113] demonstrated that the amount of fine structure due to channel tortuosity is significantly reduced if the current wave front is allowed to lengthen during its propagation along the channel.

Further smoothing should occur due to propagation effects (e.g., Le Vine *et al*. [110]).

Measured first stroke electric and magnetic fields exhibit more pronounced fine structure than subsequent strokes, a fact generally attributed to the presence of branches in first strokes. The effects of channel branches on the return-stroke radiated fields have been studied by Le Vine and Meneghini [108] and Vecchi *et al*. [115], who used the TL and MTLE return-stroke models, respectively.

Strawe [12] claims that in his distributed-circuit model the channel tortuosity is taken into account in determining the L and C values. On the other hand, Bazelyan [116] argues that the channel tortuosity has little effect on L and C, but can significantly increase R due to a tortuous path's being longer than a straight one for the same distance between the path's ends. Podgorski and Landt [22] use a linear piecewise approximation in their electromagnetic model to simulate a 3-D lightning channel of arbitrary shape including branches.

D. Propagation Effects

If the observation point of the lightning fields is located on the ground surface, and the ground is assumed to be perfectly conducting, only two field components, the vertical electric field and the azimuthal magnetic field are present, as discussed above. The horizontal electric field component is zero as required by the boundary condition on the surface of a perfect conductor. At an observation point above a perfectly conducting ground, a nonzero horizontal electric field component exists. A horizontal electric field exists both above ground and on (and below) its surface in the case of a finite ground conductivity. Propagation effects include the preferential attenuation of the higher frequency components in the vertical electric field and azimuthal magnetic field waveforms and the appearance of a horizontal (radial) electric field which can be viewed as producing the radial current flow and resultant ohmic losses in the earth. A good review of the literature on the effects of finite ground conductivity on lightning electric and magnetic fields is given by Rachidi *et al*. [117].

Two approximate equations, namely the wavetilt formula (Zenneck [118]) and the Cooray–Rubinstein formula (Cooray [119]; Rubinstein [120]), both in the frequency domain, are commonly used for the computation of the horizontal electric field in air within 10 m or so of a finitely conducting earth. The term "wavetilt" originates from the fact that when a plane electromagnetic wave propagates over a finitely conducting ground, the total electric field vector at the surface is tilted from the vertical because of the presence of a nonzero horizontal (radial) electric field component. The tilt is in the direction of propagation if the vertical electric field component is directed upward and in the direction opposite to the propagation direction if the vertical electric field component is directed downward with the vertical component of the Poynting vector being directed into the ground in both cases.

The wavetilt formula states that for a plane wave the ratio of the Fourier transform of the horizontal electric field $E_r(j\omega)$ to that of the vertical electric field $E_z(j\omega)$ is equal to the ratio of the propagation constants in the air and in the ground (Zenneck [118]). Therefore

$$E_r(j\omega) = E_z(j\omega)\frac{1}{\sqrt{\varepsilon_{\rm rg} + \sigma_g/(j\omega\varepsilon_0)}} \tag{10}$$

where σ_g and $\varepsilon_{\rm rg}$ are the conductivity and relative permittivity of the ground, respectively, and ω is the angular frequency. The formula is a special case (valid for grazing incidence) of the theory of the reflection of electromagnetic waves off a conducting surface and, hence, is a reasonable approximation only for relatively distant lightning or for the early microseconds of close lightning when the return-stroke wavefront is near ground. $E_z(j\omega)$ is typically computed assuming a perfectly conducting ground or is measured.

The Cooray–Rubinstein equation is expressed as follows (Cooray [119], Rubinstein [120]):

$$E_r(r,z,j\omega) = E_{rp}(r,z,j\omega) - H_{\phi p}(r,0,j\omega)\frac{c\mu_0}{\sqrt{\varepsilon_{\rm rg} + \sigma_g/(j\omega\varepsilon_0)}} \tag{11}$$

where μ_0 is the permeability of free-space $E_{rp}(r,z,j\omega)$ and $H_{\phi p}(r,0,j\omega)$ are the Fourier transforms of the horizontal electric field at height z above ground and the azimuthal magnetic field at ground level, respectively, both computed for the case of a perfectly conducting ground. The second term is equal to zero for $\sigma_g \to \infty$ and becomes increasingly important as σ_g decreases. A generalization of the Cooray–Rubinstein formula has been offered by Wait [121].

Cooray and Lundquist [122] and Cooray [123], using an analytical time-domain attenuation function proposed by Wait [124], have calculated the effects of a finitely conducting earth in modifying the initial portion of the vertical electric field waveforms from the values expected over an infinitely conducting earth. The results are in good agreement with measurements of Uman *et al*. [125] and Lin *et al*. [72]. Uman *et al*. [125] observed that zero-to-peak risetimes for typical strokes increase of the order of 1 μs in propagating 200 km across Florida soil. Lin *et al*. [72] reported that normalized peak fields were typically attenuated 10% in propagating over 50 km of Florida soil and 20% in propagating 200 km. For distances greater than a few hundred meters minimal distortion of the fast transition in the field wavefront and other rapidly changing portions of the measured field waveforms can be assured only when the propagation path is almost entirely over salt water, a relatively good conductor. Nevertheless, Ming and Cooray [126] found from theory that for frequencies higher than about 10 MHz the attenuation caused by the rough ocean surface can be significant. For the worst cases considered, they reported that the peak of the radiation field derivative was attenuated by about 35% in propagating 50–100 km. Cooray and Ming [127] theoretically considered propagation partly over sea and partly over land and found that the propagation effects on the electric radiation field derivative were significant unless the length of the land portion of the propagation path is less than a few tens of meters. The propagation effects on the peak of the radiation field can be neglected if the length of the overland propagation path is less than about 100 m.

ACKNOWLEDGMENT

The authors would like to thank C. Baum who read the manuscript and provided helpful comments and suggestions. They would also like to thank two anonymous reviewers.

REFERENCES

[1] R. Lundholm, "Induced overvoltage-surges on transmission lines and their bearing on the lightning performance at medium voltage networks," *Trans. Chalmers Univ. Technol.*, no. 120, p. 117, 1957.

[2] H. Norinder and O. Dahle, "Measurements by frame aerials of current variations in lightning discharges," *Arkiv Mat. Astron. Fysik*, vol. 32A, pp. 1–70, 1945.

[3] M. J. Master, M. A. Uman, Y. T. Lin, and R. B. Standler, "Calculations of lightning return stroke electric and magnetic fields above ground," *J. Geophys. Res.*, vol. 86, pp. 12,127–12,132, 1981.

[4] F. Rachidi and C. A. Nucci, "On the Master, Uman, Lin, Standler and the modified transmission line lightning return stroke current models," *J. Geophys. Res.*, vol. 95, pp. 20, 389–20, 393, 1990.

[5] M. N. Plooster, "Shock waves from line sources. Numerical solutions and experimental measurements," *Phys. Fluids*, vol. 13, pp. 2665–2675, 1970.

[6] ——, "Numerical simulation of spark discharges in air," *Phys. Fluids*, vol. 14, pp. 2111–2123, 1971.

[7] ——, "Numerical model of the return stroke of the lightning discharge," *Phys. Fluids*, vol. 14, pp. 2124–2133, 1971.

[8] S. I. Drabkina, "The theory of the development of the spark channel," *J. Exper. Theoret. Phys.*, vol. 21, pp. 473–483, 1951 (Engl. transl. AERE LIB/Trans. 621, Harwell, Berkshire, U.K.).

[9] S. I. Braginskii, "Theory of the development of a spark channel," *Sov. Phys. JETP*, vol. 34, pp. 1068–1074, 1958 (Engl. transl.).

[10] R. D. Hill, "Channel heating in return stroke lightning," *J. Geophys. Res.*, vol. 76, pp. 637–645, 1971.

[11] ——, "Energy dissipation in lightning," *J. Geophys. Res.*, vol. 82, pp. 4967–4968, 1977.

[12] D. F. Strawe, "Non-linear modeling of lightning return strokes," in *Proc. Fed. Aviat. Administra./Florida Inst. Technol. Workshop Grounding Lightning Technol.*, Melbourne, FL, Mar. 1979, pp. 9–15, Rep. FAA-RD-79-6.

[13] A. H. Paxton, R. L. Gardner, and L. Baker, "Lightning return stroke: A numerical calculation of the optical radiation," *Phys. Fluids*, vol. 29, pp. 2736–2741, 1986.

[14] ——, "Lightning return stroke: A numerical calculation of the optical radiation" in *Lightning Electromagnetics*. New York: Hemisphere, 1990, pp. 47–61.

[15] A. S. Bizjaev, V. P. Larionov, and E. H. Prokhorov, "Energetic characteristics of lightning channel," in *Proc. 20th Int. Conf. Lightning Protect.*, Interlaken, Switzerland, Sept. 1990, pp. 1.1/1–1.1/3.

[16] E. I. Dubovoy, V. I. Pryazhinsky, and G. I. Chitanava, "Calculation of energy dissipation in lightning channel," *Meteorologiya i Gidrologiya*, no. 2, pp. 40–45, 1991.

[17] E. I. Dubovoy, V. I. Pryazhinsky, and V. E. Bondarenko, "Numerical modeling of the gasodynamical parameters of a lightning channel and radio-sounding reflection," *Izvestiya AN SSSR-Fizika Atmosfery i Okeana*, vol. 27, pp. 194–203, 1991.

[18] E. I. Dubovoy, M. S. Mikhailov, A. L. Ogonkov, and V. I. Pryazhinsky, "Measurement and numerical modeling of radio sounding reflection from a lightning channel," *J. Geophys. Res.*, vol. 100, pp. 1497–1502, 1995.

[19] E. P. Krider, G. A. Dawson, and M. A. Uman, "The peak power and energy dissipation in a single-stroke lightning flash," *J. Geophys. Res.*, vol. 73, pp. 3335–3339, 1968.

[20] M. A. Uman, *The Lightning Discharge*. San Diego, CA: Academic, 1987.

[21] J. E. Borovsky, "Lightning energetics: Estimates of energy dissipation in channels, channel radii, and channel-heating risetimes," *J. Geophys. Res.*, vol. 103, pp. 11 537–11 553, 1998.

[22] A. S. Podgorski and J. A. Landt, "Three dimensional time domain modeling of lightning," *IEEE Trans. Power Del.*, vol. PWRD-2, pp. 931–938, July 1987.

[23] R. Moini, V. A. Rakov, M. A. Uman, and B. Kordi, "An antenna theory model for the lightning return stroke," in *Proc. 12th Int. Zurich Symp. Electromagnetic Compat.*, Zurich, Switzerland, Feb. 1997, pp. 149–152.

[24] M. N. O. Sadiku, *Elements of Electromagnetics*. Orlando, FL: Sounders College Press, 1994.

[25] C. R. Paul, *Analaysis of Milticonductor Transmission Lines*. New York: Wiley, 1994.

[26] J. E. Borovsky, "An electrodynamic description of lightning return strokes and dart leaders: Guided wave propagation along conducting cylindrical channels," *J. Geophys. Res.*, vol. 100, pp. 2697–2726, 1995.

[27] A. K. Agrawal, H. J. Price, and S. H. Gurbaxani, "Transient response of multiconductor transmission lines excited by a nonuniform electromagnetic field," *IEEE Trans. Electromagn. Compat.*, vol. EMC-22, pp. 119–129, May 1980.

[28] V. A. Rakov, "Some inferences on the propagation mechanisms of dart leaders and return strokes," *J. Geophys. Res.*, vol. 103, pp. 1879–1887, 1998.

[29] B. N. Gorin, "Mathematical modeling of the lightning return stroke," *Elektrichestvo*, no. 4, pp. 10–16, 1985.

[30] C. E. Baum and L. Baker, "Analytic return-stroke transmission-line model," in *Lightning Electromagnetics*. New York: Hemisphere, 1990, pp. 17–40.

[31] C. E. Baum, "Return-stroke initiation," in *Lightning Electromagnetics*. New York: Hemisphere, 1990, pp. 101–114.

[32] G. N. Oetzel, "Computation of the diameter of a lightning return stroke," *J. Geophys. Res.*, vol. 73, pp. 1889–1896, 1968.

[33] G. H. Price and E. T. Pierce, "The modeling of channel current in the lightning return stroke," *Radio Sci.*, vol. 12, pp. 381–388, 1977.

[34] P. F. Little, "Transmission line representation of a lightning return stroke," *J. Phys. D: Appl. Phys.*, vol. 11, pp. 1893–1910, 1978.

[35] N. Takagi and T. Takeuti, "Oscillating bipolar electric field changes due to close lightning return strokes," *Radio Sci.*, vol. 18, pp. 391–398, 1983.

[36] D. M. Jordan and M. A. Uman, "Variation in light intensity with height and time from subsequent lightning return strokes," *J. Geophys. Res.*, vol. 88, pp. 6555–6562, 1983.

[37] D. W. Quinn, "Modeling of lightning," *Math. Comput. Simulat.*, vol. 29, pp. 107–118, 1987.

[38] E. M. Bazelyan, B. N. Gorin, and V. I. Levitov, *Physical and Engineering Foundations of Lightning Protection*. Leningrad, USSR: Gidrometeoizdat, 1978.

[39] M. A. da F. Mattos and C. Christopoulos, "A nonlinear transmission line model of the lightning return stroke," *IEEE Trans. Electromagn. Compat.*, vol. 30, pp. 401–406, Aug. 1988.

[40] ——, "A model of the lightning channel, including corona, and prediction of the generated electromagnetic fields," *J. Phys. D Appl. Phys.*, vol. 23, pp. 40–46, 1990.

[41] M. V. Kostenko, "Electrodynamic characteristics of lightning and their influence on disturbances of high-voltage lines," *J. Geophys. Res.*, vol. 100, pp. 2739–2747, 1995.

[42] L. Baker, "Return-stroke transmission line model," in *Lightning Electromagnetics*. New York: Hemisphere, 1990, pp. 63–74.

[43] R. Thottappillil, V. A. Rakov, and M. A. Uman, "Distribution of charge along the lightning channel: Relation to remote electric and magnetic fields and to return stroke models," *J. Geophys. Res.*, vol. 102, pp. 6887–7006, 1997.

[44] V. A. Rakov, "Lightning electromagnetic fields: Modeling and measurements," in *Proc. 12th Int. Zurich Symp. Electromagn. Compat.*, Zurich, Switzerland, Feb. 1997, pp. 59–64.

[45] V. A. Rakov and A. A. Dulzon, "A modified transmission line model for lightning return stroke field calculations," in *Proc. 9th Int. Zurich. Symp. Electromagn. Compat.*, Zurich, Switzerland, Mar. 1991, pp. 229–235.

[46] M. A. Uman and D. K. McLain, "Magnetic field of the lightning return stroke," *J. Geophys. Res.*, vol. 74, pp. 6899–6910, 1969.

[47] V. A. Rakov and A. A. Dulzon, "Calculated electromagnetic fields of lightning return stroke," *Tekh. Elektrodinam.*, no. 1, pp. 87–89, 1987.

[48] C. A. Nucci, C. Mazzetti, F. Rachidi, and M. Ianoz, "On lightning return stroke models for LEMP calculations," in *Proc. 19th Int. Conf. Lightning Protection*, Graz, Austria, Apr. 1988.

[49] C. E. R. Bruce and R. H. Golde, "The lightning discharge," *J. Inst. Elect. Eng.—Pt. 2*, vol. 88, pp. 487–520, 1941.

[50] F. Heidler, "Traveling current source model for LEMP calculation," in *Proc. 6th Int. Zurich Symp. Electromagn. Compat.*, Zurich, Switzerland, Mar. 1985, pp. 157–162.

[51] J. A. Leise and W. L. Taylor, "A transmission line model with general velocities for lightning," *J. Geophys. Res.*, vol. 82, pp. 391–396, 1977.

[52] A. A. Dulzon and V. A. Rakov, "Estimation of errors in lightning peak current measurements by frame aerials," *Izvestiya VUZov SSSR-Energetika*, no. 11, pp. 101–104, 1980.

[53] G. Diendorfer and M. A. Uman, "An improved return stroke model with specified channel-base current," *J. Geophys. Res.*, vol. 95, pp. 13,621–13,644, 1990.

[54] R. Thottappillil, D. K. Mclain, M. A. Uman, and G. Diendorfer, "Extention of the Diendorfer-Uman lightning return stroke model to the case of a variable upward return stroke speed and a variable downward discharge current speed," *J. Geophys. Res.*, vol. 96, pp. 17 143–17 150, 1991.

[55] R. Thottappillil and M. A. Uman, "A lightning return-stroke model with height-variable discharge time constant," *J. Geophys. Res.*, vol. 99, pp. 22 773–22 780, 1994.
[56] M. A. Uman, D. K. Mclain, and E. P. Krider, "The electromagnetic radiation from a finite antenna," *Amer. J. Phys.*, no. 43, pp. 33–38, 1975.
[57] C. A. Nucci, G. Diendorfer, M. A. Uman, F. Rachidi, M. Ianoz, and C. Mazzetti, "Lightning return stroke current models with specified channel-base current: A review and comparison," *J. Geophys. Res.*, vol. 95, pp. 20 395–20 408, 1990.
[58] V. Cooray, "A model for subsequent return strokes," *J. Electrostat.*, vol. 30, pp. 343–354, 1993.
[59] F. Heidler and C. Hopf, "Lightning current and lightning electromagnetic impulse considering current reflection at the earth's surface," in *Proc. 22nd Int. Conf. Lightning Protection*, Budapest, Hungary, 1994, Paper R4-05.
[60] ——, "Influence of channel-base current and current reflections on the initial and subsidiary lightning electromagnetic field peak," in *Proc. 1995 Int. Aerosp. Ground Conf. Lightning Static Electricity*, Williamsburg, VA, 1995, pp. 18/1–18/10.
[61] ——, "On the influence of the ground conductivity, the current reflections and the current generation on the electric field in a general TCS-model," in *Proc. 23rd Int. Conf. Lightning Protection*, Florence, Italy, 1996, pp. 316–321.
[62] J. M. Cvetic and B. V. Stanic, "LEMP calculation using an improved return stroke model," in *Proc. 12th Int. Zurich Symp. Electromagn. Compat.*, Zurich, Switzerland, Feb. 1997, pp. 77–82.
[63] R. E. Orville, "A high-speed time-resolved spectroscopic study of the lightning return stroke: Part I—A qualitative analysis," *J. Atmospheric Sci.*, vol. 25, pp. 827–838, 1968.
[64] ——, "A high-speed time-resolved spectroscopic study of the lightning return stroke: Part II—A quantitative analysis," *J. Atmospheric Sci.*, vol. 25, pp. 839–851, 1968b.
[65] ——, "A high-speed time-resolved spectroscipic study of the lightning return stroke: Part III—A time-dependent model," *J. Atmospheric Sci.*, vol. 25, pp. 852–856, 1968.
[66] C. Guo and E. P. Krider, "The optical and radiation field signatures produced by lightning return strokes," *J. Geophys. Res.*, vol. 87, pp. 8913–8922, 1982.
[67] ——, "The optical power radiated by lightning return strokes," *J. Geophys. Res.*, vol. 88, pp. 8621–8622, 1983.
[68] A. H. Paxton, L. Baker, and R. L. Gardner, "Reply to comments of Hill," *Phys. Fluids*, vol. 30, pp. 2586–2587, 1987.
[69] V. Cooray, "Energy dissipation in lightning flashes," *J. Geophys. Res.*, vol. 102, pp. 21,401–21,410, 1997.
[70] A. A. Few, "Power spectrum of thunder," *J. Geophys. Res.*, vol. 74, pp. 6926–6934, 1969.
[71] A. A. Few, "Acoustic radiations from lightning," in *Handbook of Atmospheric Electrodynamics*. Boca Raton, FL: CRC, 1995, vol. II, pp. 1–31.
[72] Y. T. Lin, M. A. Uman, J. A. Tiller, R. D. Brantley, W. H. Beasley, E. P. Krider, and C. D. Weidman, "Characterization of lightning return stroke electric and magnetic fields from simultaneous two-station measurements," *J. Geophys. Res.*, vol. 84, pp. 6307–6314, 1979.
[73] M. A. Uman, V. A. Rakov, J. A. Versaggi, R. Thottappillil, A. Eybert-Berard, L. Barret, J.-P. Berlandis, B. Bador, P. P. Barker, S. P. Hnat, J. P. Oravsky, T. A. Short, C. A. Warren, and R. Bernstein, "Electric fields close to triggered lightning," in *Proc. EMC'94 ROMA, Int. Symp. Electromagn. Compat.*, Rome, Italy, Sept. 1994, pp. 33–37.
[74] M. A. Uman, V. A. Rakov, K. J. Rambo, T. W. Vaught, M. I. Fernandez, D. J. Cordier, R. M. Chandler, R. Bernstein, and C. Golden, "Triggered-lightning experiments at Camp Blanding, FL (1993–1995)," *Trans. Inst. Elect. Eng. Japan*, vol. 117-B, no. 4, pp. 446–452, 1997.
[75] V. A. Rakov, M. A. Uman, K. J. Rambo, M. I. Fernandez, R. J. Fisher, G. H. Schnetzer, R. Thottappillil, A. Eybert-Berard, J. P. Berlandis, P. Lalande, A. Bonamy, P. Laroche, and A. Bondiou-Clergerie, "New insights into lightning processes gained from triggered-lightning experiments in Florida and Alabama," *J. Geophys. Res.*, vol. 102, pp. 14 117–14 130, 1998.
[76] R. Thottappillil, M. A. Uman, and G. Diendorfer, "Influence of channel base current and varying return stroke speed on the calculated fields of three important return stroke models," in *Proc. 1991 Int. Conf. Lightning Static Electricity*, Cocoa Beach, FL, Apr. 1991, pp. 118.1–118.9.
[77] W. H. Beasley, M. A. Uman, and P. L. Rustan, "Electric fields preceding cloud to ground lightning flashes," *J. Geophys. Res.*, vol. 87, pp. 4884–4902, 1982.
[78] R. Thottappillil and M. A. Uman, "Comparison of lightning return-stroke models," *J. Geophys. Res.*, vol. 98, pp. 22,903–22,914, 1993.
[79] J. C. Willett, J. C. Bailey, V. P. Idone, A. Eybert-Berard, and L. Barret, "Submicrosecond intercomparison of radiation fields and currents in triggered lightning return strokes based on the transmission-line model," *J. Geophys. Res.*, vol. 94, pp. 13,275–13,286, 1989.
[80] Y. T. Lin, M. A. Uman, and R. B. Standler, "Lightning return stroke models," *J. Geophys. Res.*, vol. 85, pp. 1571–1583, 1980.
[81] P. R. Krehbiel, M. Brook, and R. McCrory, "An analysis of the charge structure of lightning discharges to the ground," *J. Geophys. Res.*, vol. 84, pp. 2432–2456, 1979.
[82] V. A. Rakov, M. A. Uman, D. M. Jordan, and C. A. Priori III, "Ratio of leader to return-stroke electric field change for first and subsequent lightning strokes," *J. Geophys. Res.*, vol. 95, pp. 16,579–16,587, 1990.
[83] X. M. Shao, P. R. Krehbiel, R. J. Thomas, and W. Rison, "Radio interferometric observations of cloud-to-ground lightning phenomena in Florida," *J. Geophys. Res.*, vol. 100, pp. 2749–2783, 1995.
[84] S. Guerrieri, C. A. Nucci, F. Rachidi, and M. Rubinstein, "On the influence of elevated strike objects on directly measured and indirectly estimated lightning currents," *IEEE Trans. Power Delivery*, to be published.
[85] F. Rachidi, W. Janischewskyj, A. M. Hussein, C. A. Nucci, S. Guerrieri, and J. S. Chang, "Electromagnetic fields radiated by lightning return strokes to high towers," in *Proc. 24th Int. Conf. Lightning Protection*, Birmingham, U.K., Sept. 1998, pp. 23–28.
[86] D. Wang, N. Takagi, T. Watanabe, V. A. Rakov, and M. A. Uman, "Observed leader stepping return-stroke in the bottom 400 m of the rocket-triggered lightning channel," *J. Geophys. Res.*, to be published.
[87] S. Yokoyama, K. Miyake, T. Suzuki, and S. Kanao, "Winter lightning on Japan sea coast-development of measuring system on progressing feature of lightning discharge," *IEEE Trans. Power Delivery*, vol. 5, pp. 1418–1425, July 1990.
[88] C. Leteinturier, C. Weidman, and J. Hamelin, "Current and electric field derivatives in triggered lightning return strokes," *J. Geophys. Res.*, vol. 95, pp. 811–828, 1990.
[89] V. Cooray, "Derivation of return stroke parameters from the electric and magnetic field derivatives," *Geophys. Res. Lett.*, vol. 16, pp. 61–64, 1989.
[90] V. A. Rakov, R. Thottappillil, and M. A. Uman, "On the empirical formula of Willett et al. relating lightning return stroke peak current and peak electric field," *J. Geophys. Res.*, vol. 97, pp. 11 527–11 533, 1992.
[91] K. M. L. Srivastava, "Return stroke velocity of a lightning discharge," *J. Geophys. Res.*, vol. 71, pp. 1283–1286, 1966.
[92] B. F. J. Schonland, "The lightning discharge," *Handbuch der Physik*. Berlin, Germany: Springer-Verlag, 1956, no. 22, pp. 576–628.
[93] C. F. Wagner and A. R. Hileman, "The lightning stroke," *Amer. Inst. Elect. Eng. (AIEE) Trans.* vol. 77, pt. 3, pp. 229–242, 1958.
[94] M. A. Uman, D. K. McLain, R. J. Fisher, and E. P. Krider, "Currents in Florida lightning return strokes," *J. Geophys. Res.*, vol. 78, pp. 3530–3537, 1973.
[95] J. C. Willett, V. P. Idone, R. E. Orville, C. Leteinturier, A. Eybert-Berard, L. Barret, and E. P. Krider, "An experimental test of the "transmission-line model" of electromagnetic radiation from triggered lightning return strokes," *J. Geophys. Res.*, vol. 93, pp. 3867–3878, 1988.
[96] D. Wang, V. A. Rakov, M. A. Uman, N. Takagi, T. Watanabe, D. Crawford, K. J. Rambo, G. H. Schnetzer, R. J. Fisher, and Z. I. Kawasaki, "Attachment process in rocket-triggered lightning strokes," *J. Geophys. Res.*, to be published.
[97] M. Rubinstein, F. Rachidi, M. A. Uman, R. Thottappillil, V. A. Rakov, and C. A. Nucci, "Characterization of vertical electric fields 500 m and 30 m from triggered lightning," *J. Geophys. Res.*, vol. 100, pp. 8863–8872, 1995.
[98] D. M. Le Vine and J. C. Willett, "Comments on the transmission-line model for computing radiation from lightning," *J. Geophys. Res.*, vol. 97, pp. 2601–2610, 1992.
[99] R. Thottappillil, M. A. Uman, and V. A. Rakov, "Treatment of retardation effects in calculating the radiated electromagnetic fields from the lightning discharge," *J. Geophys. Res.*, vol. 103, pp. 9003–9013, 1998.
[100] M. Rubinstein and M. A. Uman, "On the radiation field turn-on term associated with traveling current discontinuities in lightning," *J. Geophys. Res.*, vol. 95, pp. 3711–3713, 1990.
[101] ——, "Transient electric and magnetic fields associated with establishing a finite electrostatic dipole revisited," *IEEE Trans. Electromagn. Compat.*, vol. 33, pp. 312–320, Nov. 1991.
[102] E. P. Krider, "On the electromagnetic fields, Poynting vector, and peak power radiated by lightning return strokes," *J. Geophys. Res.*, vol. 97, pp. 15 913–15 917, 1992.
[103] L. E. Salanave, *Lightning and Its Spectrum*. Tucson, AZ: Univ. Arizona Press, 1980.

[104] R. D. Hill, "Analysis of irregular paths of lightning channels," *J. Geophys. Res.*, vol. 73, pp. 1897–1906, 1968.
[105] ———, "Electromagnetic radiation from erratic paths of lightning strokes," *J. Geophys. Res.*, vol. 74, pp. 1922–1929, 1969.
[106] V. P. Idone, "Microscale tortuosity and its variation as observed in triggered lightning channels," *J. Geophys. Res.*, vol. 100, pp. 22 943–22 956, 1995.
[107] D. M. Le Vine and J. C. Willett, "The influence of channel geometry on the fine scale structure of radiation from lightning return strokes," *J. Geophys. Res.*, vol. 100, pp. 18,629–18,638, 1995.
[108] D. M. Le Vine and R. Meneghini, "Simulation of radiation from lightning return strokes: The effect of tortuosity," *Radio Sci.*, vol. 13, pp. 801–809, 1978.
[109] ———, "Electromagnetic fields radiated from a lightning return stroke: Application of an exact solution of Maxwell's equations," *J. Geophys. Res.*, vol. 83, pp. 2377–2384, 1978.
[110] D. M. Le Vine, L. Gesell, and M. Kao, "Radiation from lightning return strokes over a finitely conducting earth," *J. Geophys. Res.*, vol. 91, pp. 11 897–11 908, 1986.
[111] D. M. Le Vine and M. Kao, "The effects of current risetime on radiation from tortuous lightning channels," in *Proc. 8th Int. Conf. Atmospheric Electricity*, Uppsala, Sweden, June 1988, pp. 509–514.
[112] R. L. Gardner, "Effect of the propagation path of lightning—induced transient fields," in *Lightning Electromagn.*. New York: Hemisphere, pp. 139–153, 1990.
[113] V. Cooray and R. E. Orville, "The effects of variation of current amplitude, current risetime, and return stroke velocity along the return stroke channel on the electromagnetic fields generated by return strokes," *J. Geophys. Res.*, vol. 95, pp. 18 617–18 630, 1990.
[114] G. Vecchi, D. Labate, and F. Canavero, "Fractal approach to lightning radiation on a tortuous channel," *Radio Sci.*, vol. 29, pp. 691–704, 1994.
[115] G. Vecchi, R. E. Zich, and F. C. Canavero, "A study of the effect of channel branching on lightning radiation," in *Proc. 12th Int. Zurich Symp. Electromagn. Compat.*, Zurich, Switzerland, Feb. 1997, pp. 65–70.
[116] E. M. Bazelyan, "Waves of ionization in lightning discharge," *Plasma Phys. Rep.*, vol. 21, pp. 470–478, 1995.
[117] F. Rachidi, C. A. Nucci, M. Ianoz, and C. Mazzetti, "Influence of a lossy ground on lightning-induced voltages on overhead lines," *IEEE Trans. Electromagn. Compat.*, vol. 38, pp. 250–264, Aug. 1996.
[118] J. Zenneck, *Wireless Telegraphy*. New York: McGraw-Hill, 1915 (Engl. transl., A.E. Seelig).
[119] V. Cooray, "Horizontal fields generated by return stroke strokes," *Radio Sci.*, vol. 27, pp. 529–537, 1992.
[120] M. Rubinstein, "An approximate formula for the calculation of the horizontal electric field from lightning at close, intermediate, and long range," *IEEE Trans. Electromagn. Compat.*, vol. 38, pp. 531–535, 1996.
[121] J. R. Wait, "Concerning the horizontal electric field of lightning," *IEEE Trans. Electromagn. Compat.*, vol. 39, p. 186, May 1997.
[122] V. Cooray and S. Lundquist, "Effects of propagation on the risetimes and the initial peaks of radiation peaks from return strokes," *Radio Sci.*, vol. 18, pp. 409–415, 1983.
[123] V. Cooray, "Effects of propagation on the return stroke radiation fields," *Radio Sci.*, vol. 22, pp. 757–768, 1987.
[124] J. R. Wait, "Transient fields of a vertical dipole over a homogeneous curved ground," *Canadian J. Phys.*, vol. 34, pp. 27–35, 1956.
[125] M. A. Uman, C. E. Swanberg, J. A. Tiller, Y. T. Lin, and E. P. Krider, "Effects of 200 km propagation on lightning return stroke electric fields," *Radio Sci.*, vol. 11, pp. 985–990, 1976.
[126] Y. Ming and V. Cooray, "Propagation effects caused by a rough ocean surface on the electromagnetic fields generated by lightning return strokes," *Radio Sci.*, vol. 29, pp. 73–85, 1994.
[127] V. Cooray and Y. Ming, "Propagation effects on the lightning-generated electromagnetic fields for homogeneous and mixed sea-land paths," *J. Geophys. Res.*, vol. 99, pp. 10 641–10 652, 1994.

Vladimir A. Rakov (SM'96) received the M.S. and Ph.D. degrees from Tomsk Polytechnical University (Tomsk Polytechnic), Tomsk, Russia, in 1977 and 1983, respectively.

From 1977 to 1979, he worked as an Assistant Professor of electrical engineering at Tomsk Polytechnic. In 1978 he became involved in lightning research at the High Voltage Research Institute, a division of Tomsk Polytechnic, where from 1984 to 1994 he held the position of Director of the Lightning Research Laboratory. From 1988 to 1989 he spent a ten-month sabbatical at the Lightning Research Laboratory, University of Florida, Gainesville. In 1991, he joined the faculty of the Department of Electrical and Computer Engineering there. He is currently a Professor in the Department of Electrical and Computer Engineering at the same university. He is the author or coauthor of over 30 patents and over 170 papers and technical reports on various aspects of lightning, with over 60 papers being published in reviewed journals.

Dr. Rakov received the rank of Senior Scientist in High Voltage Engineering in 1985. He was named an Inventor of the USSR in 1986 and received a Silver Medal from the National Exhibition of Technological Achievements, USSR, in 1987. He is a member of the American Geophysical Union (AGU), the American Meteorological Society (AMS), the AGU Committee on Atmospheric and Space Electricity (CASE), and the CIGRE Working Group 33.01 "Lightning." He is also Chairman of the Technical Committee on Lightning (TC-10) of the biennial International Zurich Symposium on Electromagnetic Compatibility.

Martin A. Uman (SM'73–F'88) received the B.S., M.S., and Ph.D. degrees from Princeton University, Princeton, NJ, in 1957, 1959, and 1961, respectively.

From 1961 to 1964, he was an Associate Professor of Electrical Engineering, University of Arizona, Tucson. He joined the faculty of University of Florida, Gainesville, in 1971, after working for seven years as a Fellow Physicist at Westinghouse Research Laboratories, Pittsburgh, PA. He cofounded and served as President of Lightning Location and Protection Inc. (LLP) from 1975 to 1985. He is currently Professor and Chair of the Department of Electrical and Computer Engineering, University of Florida. He has written three books on the subject of lightning (two now in revised second editions), as well as a book on plasma physics, and ten book chapters and encyclopedia articles on lightning. He has published over 130 papers in reviewed journals and over 140 articles and reports in unreviewed publications. He holds five patents—four in the area of lightning detection.

Dr. Uman is the recipient of the 1996 IEEE Heinrich Hertz Medal for "outstanding contributions to the understanding of lightning electromagnetics and its application to lightning detection and protection." He was named the 1990 Florida Scientist of the Year by the Florida Academy of Sciences. Honored as 1988–1989 University of Florida Teacher Scholar of the Year, the highest University of Florida faculty award, he is a Fellow of the American Geophysical Union (AGU) and the American Meteorological Society (AMS). He also received NASA's 1992 and 1996 Group Achievement Award to the Galileo Probe Spacecraft Team.